UNIVERSITY OF SIENA

DEPARTMENT OF BIOTECHNOLOGY,
CHEMISTRY AND PHARMACY

DOCTORAL THESIS IN
BIOCHEMISTRY AND MOLECULAR BIOLOGY
Cycle XXXVII

Coordinator: Prof. Lorenza Trabalzini

ROLE OF KRIT1 IN THE ACQUISITION OF AGGRESSIVE PHENOTYPE IN CANCER CELLS

SCIENTIFIC-DISCIPLINARY SECTOR: BIOS-07/A

TUTOR
Prof. LORENZA TRABALZINI

PhD STUDENT
LUCREZIA PARADISI

Academic year 2023-2024

ABSTRACT

K-Rev Interaction Trapped protein-1 (KRIT1) is a scaffold protein known to form functional protein complexes involved in physiologically important signaling networks. While it is primarily recognised for its association with Cerebral Cavernous Malformations (CCMs), KRIT1 also plays critical roles in tumor formation and the acquisition of malignant phenotypes. These roles include functions in cell adhesion, cytoskeletal dynamics, and angiogenesis.

The present study investigates the involvement of KRIT1 in tumor progression and plasticity. The research focused on the potential tumor-suppressor-like properties of KRIT1, particularly in relation to invasion and migration processes. Notably, KIF1C and NS1A have been identified as novel binding partners of KRIT1. KIF1C plays a crucial role in regulating podosomes and invadopodia elongation, while NS1A contributes to the organization of the actin cytoskeleton dynamics by stabilizing actin filaments through its association with F-actin. The role of KRIT1 in tumour invasion and migration was evaluated both *in vitro* and *in vivo*. Additionally, the impact of KRIT1 loss on SRC, FAK, and RhoA/ROCK signaling pathways, as well as its involvement in cytoskeleton dynamics, was analysed. The findings of this study corroborate the role of KRIT1 as a tumor suppressor gene and reveal a correlation between its depletion and increased cancer aggressiveness.

INDEX

1. INTRODUCTION

1.1. Molecular basis of cancer

Cancer is a disease characterized by uncontrolled proliferation of transformed cells subject to evolution by natural selection (Brown et al., 2023).

Cancer cells initiate tumors and drive tumor progression forward, carrying the oncogenic and tumor suppressor mutations that define cancer as a genetic disease. Traditionally, the cancer cells within tumors have been portrayed as reasonably homogeneous cell populations until relatively late during tumor progression, when hyperproliferation combined with increased genetic instability spawn distinct clonal subpopulations (Hanahan and Weinberg, 2011). However, cancer is not only a genetic disease but rather a complex ecosystem, involving a wide range of non-cancerous cells and their multiple interactions within the tumor. As a matter of facts cancer cells orchestrate a tumor-supportive environment by recruiting and reprogramming non-cancerous host cells and by remodelling the vasculature and extracellular matrix (ECM) (De Visser and Joyce, 2023).

1.1.1. Hallmarks of cancer

Hallmarks of cancer represent capabilities that enable tumor growth and metastatic dissemination providing also solid foundation for understanding cancer biology (Hanahan and Weinberg, 2011). These capabilities include:

- Sustaining Proliferative Signaling - is the fundamental characteristic of cancer cells. It is achieved by the production of growth factors by the cancer cells; the sending of stimulatory signals to normal cells in the associated stroma to produce growth factors; increased levels of neoplastic cell surface receptors; structural changes in the receptors that make them hyperreactive to limited amounts of growth factors and facilitate ligand binding. Finally, growth factor independence may result from constitutive activation of signaling pathway components downstream of these receptors that prevent stimulation by ligand binding.
- Evading Growth Suppressors - the neoplastic cell has to bypass tumor suppressor genes. The function of these genes is to limit cell proliferation.
- Resisting Cell Death - programmed death by apoptosis is a natural barrier to neoplastic development and attenuation has been observed in those tumours that progress to high pathological grades and in those that are resistant to therapy.

Neoplastic cells can inhibit apoptosis through loss of tumour suppressors, increased expression of anti-apoptotic regulators or survival signals, and finally through down-regulation of pro-apoptotic factors.

- Enabling Replicative Immortality - cancer cells require unlimited replicative potential to generate a tumour mass. This property has been attributed to their ability to maintain telomeric DNA of sufficient length to prevent the induction of senescence or apoptosis, as telomere shortening determines the limit of replicative potential of normal cells. Telomere maintenance is mainly achieved by over-regulation of telomerase expression.

- Inducing Angiogenesis - the new vascular network associated with cancer and generated by angiogenesis supplies cancer cells with oxygen, nutrients, metabolic waste and carbon dioxide. During tumour progression, the angiogenic switch is constantly on, causing the normally quiescent vasculature to generate new vessels. The walls of these new vessels have numerous fenestrations, the basal membrane is absent in some parts and the junctions between the endothelial cells are loose, contributing to the high permeability that makes them the preferred route for metastatic spread.

- Activating Invasion and Metastasis - the process begins with the invasion of tumour cells into the blood and lymphatic vessels, followed by transit within these two systems, and then extravasation into the tissue parenchyma. At the tissue level, small nodules of cancer cells, known as micro metastases, develop into macroscopic tumors. The process of metastasis can therefore be divided into two phases: the first involves the dissemination of cancer cells from the original tumour to distant tissues, and the second involves the adaptation of the cells to the environmental conditions of the colonised tissues.

- Reprogramming Energy Metabolism - uncontrolled proliferation requires an adaptation of metabolism to fuel cell growth and division. Under aerobic conditions, normal cells convert glucose to pyruvate via glycolysis in the cytosol, then pyruvate is transferred to the mitochondria where it is oxidised to carbon dioxide. Under anaerobic conditions, however, glycolysis is enhanced, and small amounts of pyruvate enter the mitochondria. As an anomaly, neoplastic cells exhibit higher levels of glycolytic activity than healthy tissue, even in the presence of oxygen; this phenomenon was first described by Otto Warburg and is therefore called the Warburg effect.

- Evading Immune Destruction - the long-standing theory of immune surveillance proposes that cells and tissues are constantly monitored by an ever-alert immune system, and that such immune surveillance is responsible for recognizing and eliminating most incipient cancer cells and thus nascent tumors. According to this logic, solid tumors that do appear have somehow managed to avoid detection by the various arms of the immune system or have been able to limit the extent of immunological killing, thereby evading eradication (Hanahan and Weinberg, 2011).

1.1.2. Tumor microenvironment

Tumor microenvironment (TME) is a highly structured ecosystem containing cancer cells surrounded by diverse non-malignant cell types, collectively embedded in an altered, vascularized extracellular matrix (Figure 1). The TME includes a rich diversity of immune cells, cancer-associated fibroblasts (CAFs), endothelial cells (ECs), pericytes, and other cell types that vary by tissue, such as adipocytes and neurons (De Visser and Joyce, 2023). As well as non-cellular components, including soluble products such as chemokines, cytokines, growth factors, and extracellular vesicles (Xiao and Yu, 2021).
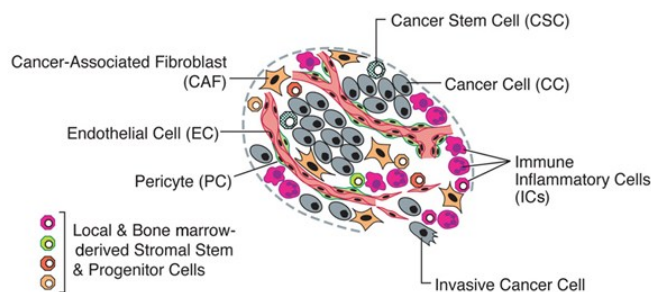

Figure 1. **Schematic representation of TME**
An assemblage of distinct cell types constitutes most solid tumors. Both the parenchyma and stroma of tumors contain distinct cell types and subtypes that collectively enable tumor growth and progression. Notably, the immune inflammatory cells present in tumors can include both tumor-promoting as well as tumor-killing subclasses (Hanahan and Weinberg, 2011)

TME has an important role in the hallmarks acquisition and maintenance and represents a therapeutical target.

Cancer steam cells (CSCs) were initially implicated in the pathogenesis of hematopoietic malignancies (Reya et al., 2001) and then years later were identified in solid tumors (Gilbertson and Rich, 2007). In some tumors, normal tissue stem cells may serve as the cells-of-origin that undergo oncogenic transformation to yield CSCs; in others, partially differentiated transit-amplifying cells, also termed progenitor cells, may suffer the initial

oncogenic transformation thereafter assuming more stem-like character. Once primary tumors have formed, the CSCs, like their normal counterparts, may self-renew as well as spawn more differentiated derivatives; in the case of neoplastic CSCs, these descendant cells form the great bulk of many tumors (Hanahan and Weinberg, 2011).

ECs are linked to the "angiogenic switch", which activates the quiescent cells, causing them to enter into a cell biological program that allows them to construct new blood vessels (Hanahan and Weinberg, 2011).

Pericytes represent a cell type with finger-like projections that wrap around the endothelial tubing of blood vessels. In normal tissues, pericytes are known to provide paracrine support signals to the normally quiescent endothelium and collaborate with the endothelial cells to synthesize the vascular basement membrane (Gaengel et al., 2009). There is a hypothesis that in tumors with poor pericyte coverage the vasculature may be more prone to permit cancer cell intravasation into the circulatory system (Raza et al., 2010).

Infiltrating cells of the immune system operate both in tumor-antagonizing and in tumor-promoting way. Between the tumor-antagonizing cells we find CD8+ cytotoxic T lymphocytes (CTLs) and natural killers (NKs), while the tumor-promoting cells include macrophage subtypes, mast cells, and neutrophils, and T and B lymphocytes. These inflammatory cells release signaling molecules that serve as effectors of their tumor-promoting actions. These include the tumor growth factor EGF, the angiogenic growth factor VEGF, other proangiogenic factors such as FGF2, chemokines, and cytokines that amplify the inflammatory state; in addition, tumor-promoting cells may produce proangiogenic and/or pro-invasive matrix-degrading enzymes, including MMP-9 and other matrix metalloproteinases, cysteine cathepsin proteases, and heparinase (Hanahan and Weinberg, 2011; Schäfer and Werner, 2008). Moreover, tumor-promoting cells are involved in the induction of tumor angiogenesis, in the stimulation of cancer cell proliferation, to facilitate, via their presence at the margins of tumors, tissue invasion, and to support the metastatic dissemination and seeding of cancer cells (Coffelt et al., 2010; Hanahan and Weinberg, 2011).

Recruited myofibroblasts and reprogrammed variants of normal tissue-derived fibroblastic cells, both defined as CAFs, have been demonstrated to enhance tumor phenotypes, notably cancer cell proliferation, angiogenesis, and invasion and metastasis (Pietras and Östman, 2010).

The tumor associated stromal cells that form TME can be supplied by proliferation of preexisting stromal cells originating in adjacent normal tissues or by recruitment of bone marrow-derived progenitor/steam cells (Hanahan and Weinberg, 2011).

1.2. Cancer cell invasion and migration

Invasion is the penetration of cells through tissue barriers such as the basement membrane and interstitial stroma. It requires adhesion, proteolysis of extracellular matrix components and migration. It occurs during normal cell morphogenesis and wound healing, as well as in malignant cells (Friedl and Wolf, 2003). Invasion and migration allow cancer cells to change their localisation within the tissue. To migrate, the cell body must change its shape and stiffness to interact with the surrounding tissue structures. The ECM provides both a substrate and a barrier to the advancing cell body. The moving cell polarises and elongates, forming cell protrusions that contain filamentous actin and a diverse set of structural and signaling proteins, leading to dynamic interactions with ECM substrates. Cell extensions include lamellipodia, filopodia, pseudopods, invadopodia or podosomes (Friedl and Wolf, 2003). Cell protrusions contact the adjacent ECM and initiate binding via adhesion molecules, notably transmembrane receptors of the integrin family. Integrins couple to the actin cytoskeleton via adaptor proteins, then become locally enriched, cluster and develop into an initial small focal complex that can grow and stabilise to form a focal contact (Hynes, 2002). Other non-integrin receptors such as CD44, discoidin receptors, CD26, immunoglobulin superfamily receptors and surface proteoglycans also interact with ECM components. The engagement of integrins and other adhesion receptors leads to the recruitment of surface proteases to attachment sites, which in turn degrade ECM components near the cell surface (Maaser et al., 1999). Before and during the development of focal contacts, actin filaments locally elongate and assemble through the action of cross-linking proteins such as α-actinin, myosin II and others. Branched actin networks beneath the inner leaflet of the plasma membrane are termed cortical actin, while cytoplasmic bundles and elongated cables of actin filaments are termed stress fibres (Cramer, 1999). Actin filament contraction is mediated by myosin II, the major motor protein in non-muscle eukaryotic cells. Myosin II-controlled stress fiber assembly and contraction are mainly induced by the small G-protein Rho and its downstream effector, Rho-associated serine/threonine kinase (ROCK). In contrast, the cortical actin network is regulated by myosin light chain kinase (MLCK) (Katoh et al., 2001; Totsukawa et al., 2000). Following disassembly of the focal complex, regions of the leading edge or the entire cell body contract, generating a traction

force that results in the gradual forward sliding of the cell body and its trailing edge (Smilenov et al., 1999). ECM-degrading enzymes, such as matrix metalloproteinases (MMPs) and cathepsins, are often upregulated in tumour cells and facilitate migration *in vitro* and dissemination and metastasis *in vivo*. Similarly, overexpression or activation of the Rac, Rho, ROCK or MLCK signaling pathways has been correlated with tumour cell migration *in vitro* and invasion and progression *in vivo*. Therefore, pharmacological inhibitors that block integrins, MMPs, ROCK or MLCK are being developed to interfere with cancer cell invasion (Friedl and Wolf, 2003).

Cancer cells can spread as individual cells, known as 'individual cell migration', or they can spread in solid cell strands, sheets, files or clusters, known as 'collective migration'. In many tumors, both individual cells and collectives are present at the same time. Whereas leukaemias, lymphomas and most solid stromal tumours, such as sarcomas, spread by individual cells, epithelial tumours often use collective migration mechanisms. In principle, the lower the stage of differentiation, the more likely the tumour is to spread by individual cells (Thiery, 2002). Individual cancer cells can disseminate via mesenchymal or ameboid modes. Ameboid movement has certain characteristics, including high-speed movement, rounded but highly deformable cell morphology and weak cell-ECM interaction, as well as a lack of intercellular adhesion and proteolytic degradation of the surrounding matrix (Wu et al., 2021). Deformability is effective for penetrating through narrow gaps of the surrounding ECM (Holle et al., 2019) and is generated by the reorganization of the cortical actin cytoskeleton (Lorentzen et al., 2011; Paluch et al., 2005). The deformation of the nucleus also maintains amoeboid cell movement; when tumour cells squeeze through pores smaller than their cell diameter, the nucleus can be deformed into a maximally compressed state (Paluch and Raz, 2013; Sanz-Moreno and Marshall, 2010). Another key motivator for cell movement is the development of bleb-like protrusions from the cell membrane to the surrounding tissue structures. These allow cells to sense the microenvironment through mechanotransduction (Paluch et al., 2005). The bleb-like protrusions and cortical actin cytoskeleton dynamics are predominantly regulated by the small GTPase RhoA and its effector ROCK. Thus, this type of migration relies predominantly on changes in cell shape rather than proteolytic degradation of the ECM (Wu et al., 2021). Mesenchymal cell migration is a typical movement pattern of fibroblasts, endothelial cells and smooth muscle cells (Chuai et al., 2012). In tumours, mesenchymal migration is often seen in tumours of connective tissue or bone marrow origin and certain poorly differentiated epithelial cancers (Sanz-Moreno et al., 2008). Epithelial-mesenchymal transition (EMT) is a key process by

which epithelial cells gain migratory ability through downregulation of epithelial markers and loss of intercellular junctions, together with upregulation of mesenchymal cell markers and increased cell motility (Aiello et al., 2018). Tumour cells that exhibit mesenchymal migration histologically show an elongated, spindle-like cell shape with the formation of pseudopod processes and filopodia. Cytoskeletal contractility, integrin-mediated ECM adhesion and proteolytic degradation of the surrounding matrix are hallmarks of mesenchymal migration. Focal adhesion kinase (FAK) and SRC kinases control cytoskeletal reorganisation and contractility by inducing the formation of focal ECM adhesions and contacts (Serrels and Frame, 2012). Membrane protrusions at the leading edge are formed in a Rac-dependent manner and cell movement is achieved with the addition of the turnover or integrin-mediated focal adhesions to the ECM. Indeed, the inactivation of Rac results in a rounded cell phenotype (Matsuoka, 2014). In contrast to amoeboid movement, mesenchymal migration depends on proteolytic degradation of the ECM. Matrix metalloproteinases and other proteases proteolytically digest ECM molecules and create cell migration pathways for disseminated cancer cells. Collective cell migration is a pattern of movement of multiple cells that maintain cell-cell connections and migrate in a coordinated manner as multicellular groups (Wu et al., 2017). The movement of these cells is dependent on actin dynamics, integrin-mediated cell-ECM adhesion and pericellular proteolysis-mediated ECM reorganisation (Wang et al., 2018). Cell-cell junctions are stabilised by cadherins (e.g. E-, N-, P-cadherin), immunoglobulin superfamily members and gap junctional cell-cell junctions (Choi et al., 2016). Collectively migrating multicellular units are groups of heterogeneous tumour cells that are polarised into a "leading edge" and a "trailing edge". Leader cells are a group of cancer cells at the invasive front and have distinctly different gene expression and morphology and proliferative, invasive and metastatic abilities compared to the follower cells at the trailing edge (Mayor and Etienne-Manneville, 2016). Leader cells control the migration of Rac-driven processes and integrin-mediated ECM adhesion (Haeger et al., 2020). In addition, MMP-14 and cathepsin B are two proteases that are overexpressed in leader cells (Wu et al., 2021) (Figure 2).

Cancer cells typically do not maintain a single mode during migration, but adapt their migration mechanisms to different environmental challenges by switching between collective and single-cell dissemination (Nagai et al., 2020). The tendency of cancer cells to switch between different motility strategies in different contexts, including those induced by therapies targeting cancer metastasis, has been reported as a potential mechanism underlying the limited efficacy of therapeutic approaches (Wu et al., 2021). The EMT, in addition has

been linked to the acquisition of treatment resistance in a variety of malignancies including solid tumors and hematologic malignancies (Ortiz et al., 2021).
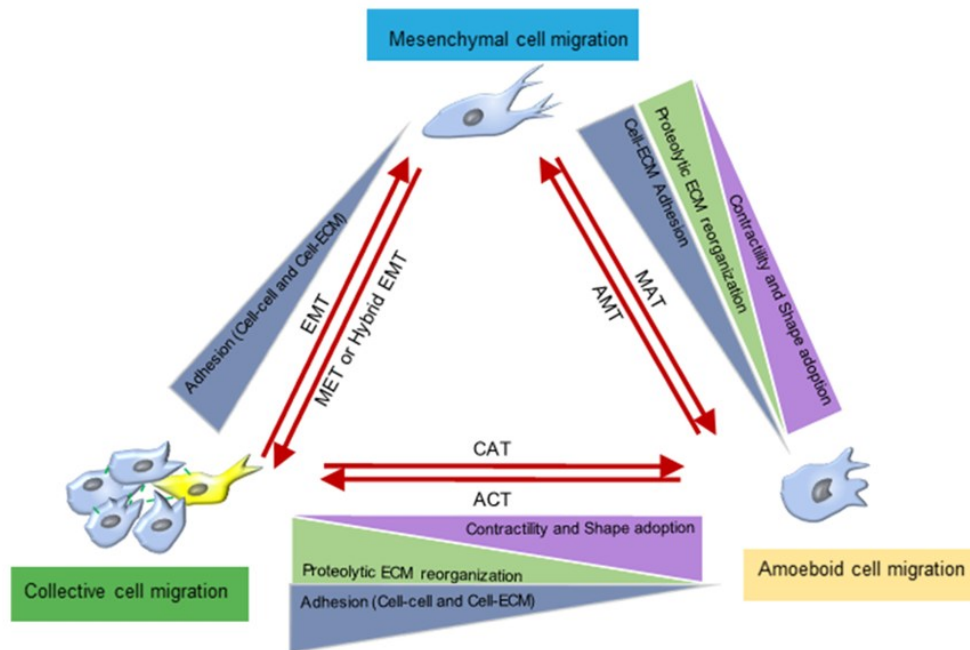

Figure 2. Plasticity of cancer cell migration modes
Cancer cells can adapt their migration mechanisms through reversible transitions between mesenchymal-amoeboid and collective-individual modes, depending on the tumor microenvironment. Single-cell plasticity, including mesenchymal-to-amoeboid (MAT) and amoeboid-to-mesenchymal (AMT) transitions, is regulated by protease activity, cell-matrix interactions, and Rho/Rac-mediated actomyosin dynamics. Reversible collective-individual transitions—such as collective-to-amoeboid, collective-to-mesenchymal, amoeboid-to-collective, and mesenchymal-to-collective—can be triggered by epithelial-to-mesenchymal transition (EMT), partial EMT, mesenchymal-to-epithelial transition (MET), collective-to-ameboid transition (CAT), or ameboid-to-collective transition (ACT), involving changes in cell-cell adhesion, cell-matrix interactions, cytoskeletal organization, or pericellular proteolysis (Wu et al., 2021)

1.2.1. Rho/ROCK signal pathways

The Rho family of small GTPases and its effector ROCK are well-established regulators of actin cytoskeleton organization and dynamics, thereby regulating cell motility and contributing to metastasis (Matsuoka, 2014).

Figure 3 provides an overview of the Rho/ROCK signaling pathway. Rho GTPases, members of the Ras superfamily of small GTP-binding proteins, are classified into three major groups: Rho, Rac, and Cdc42. Among these, RhoA, RhoB, and RhoC can interact with similar downstream effectors, while RhoE is known to exert inhibitory effects (Madaule and Axel, 1985; Riento et al., 2005). Upstream signals trigger the dissociation of GDP and the binding of GTP, causing a conformational change in the effector-binding region of the GTPase, which in turn regulates interactions with downstream targets based on nucleotide

binding or subcellular localization (Ridley, 2012). Rho GTPases function as molecular switches, converting extracellular signals into changes in the intracellular actin cytoskeleton. The activity of Rho GTPases is regulated by three key interaction molecules: guanine nucleotide exchange factors (GEFs), GTPase-activating proteins (GAPs), and guanine nucleotide dissociation inhibitors (GDIs). Rho GDIs also protect Rho GTPases from ubiquitination and degradation (Boulter et al., 2010; Doye et al., 2012). Once activated, Rho GTPases bind to effector molecules that activate downstream targets. ROCK is a serine/threonine kinase that phosphorylates downstream targets involved in cytoskeletal rearrangements. The ROCK family consists of two isoforms: ROCK1 (also known as ROCKI, p160ROCK, or ROKβ) and ROCK2 (also known as ROCKII, ROKα, or Rho-kinase). Active RhoA-GTP interacts with the C-terminal domain of ROCK, promoting the formation of stress fibres, focal adhesions, cell junctions, and regulating the cell cycle (Riento and Ridley, 2003). The ROCK family enhances myosin activity and mediates muscle contraction by phosphorylating two key substrates: myosin light chain (MLC) and myosin phosphatase 1 (MYPT1) (Somlyo et al., 2003). Several downstream targets of ROCK proteins have been identified, including intermediate filaments, ezrin/radixin/moesin (ERM) family proteins, collapsing response mediator protein 2 (CRMP2), calponin, and adducin (Matsui et al., 1998). Additionally, tau and MAP2 play roles in modulating microtubule structure and dynamics (Amano et al., 2010). Activated myosin links actin filaments to form stress fibres, which generate actomyosin forces that facilitate cell movement. LIM kinase (LIMK), another important downstream effector of Rho, phosphorylates cofilin, preventing cofilin-mediated disassembly of actin filaments (Sumi et al., 2001). Differences in activity between the two ROCK isoforms (ROCK1 and ROCK2) have been observed. One study showed that ROCK1 destabilizes the actin cytoskeleton by regulating MLC2 phosphorylation, while ROCK2 stabilizes the cytoskeleton by modulating cofilin activity (Shi et al., 2013).

The Rho subfamily, consisting of RhoA, RhoB, and RhoC, shares 85% amino acid identity. Despite this high similarity, the three isoforms exhibit distinct cellular functions (Clark et al., 2000). Overexpression of RhoA and RhoC signaling components has been observed in various human tumors, including those of the urinary tract (Kamai et al., 2003), cervix (He et al., 2010), and gastric (Liu et al., 2007). In contrast, RhoB has been shown to significantly inhibit the proliferation, migration, and invasion of gastric cancer cells (Zhou et al., 2011).
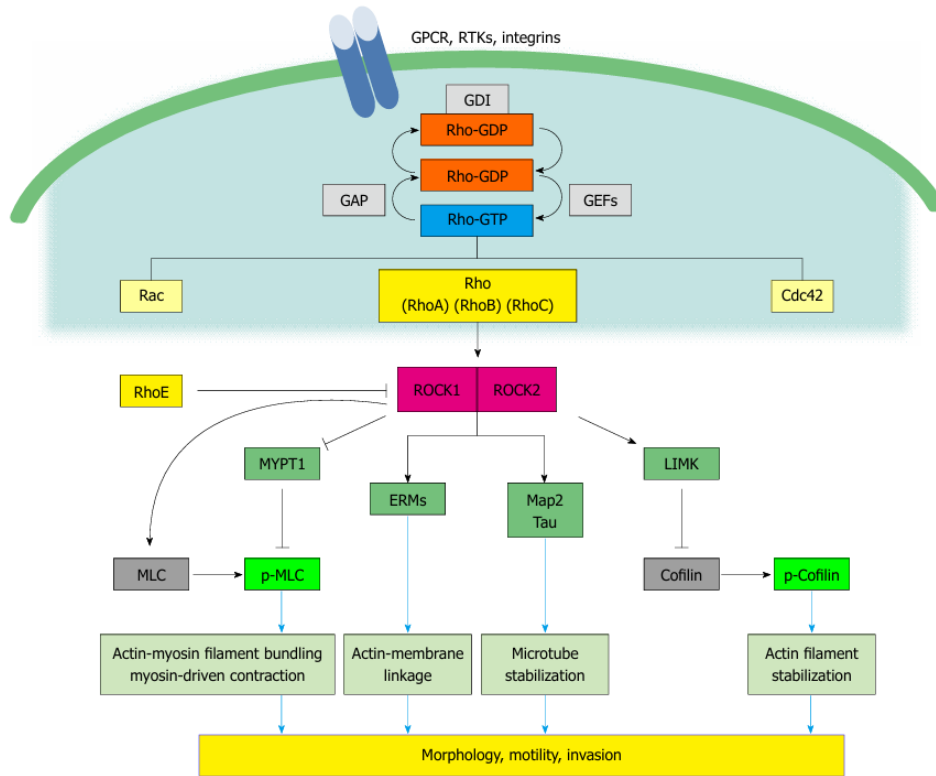
Figure 3. An overview of the Rho/Rho-associated protein kinases signaling pathway
MYPT1: Myosin phosphatase 1; MLC: Myosin light chain; ERM: Ezrin/radixin/moesin; ROCK: Rho-associated protein kinases; LIMK: LIM kinase (Matsuoka, 2014)

1.2.2. SRC pathways

SRC is a member of a family of non-receptor membrane-associated tyrosine kinases. It catalyzes the transfer of the terminal phosphate group from ATP to specific tyrosine residues on protein substrates, thereby transmitting signals from the extracellular environment into intracellular biochemical pathways. These pathways can either activate nuclear factors, leading to transcriptional responses, or target cytoplasmic components, resulting in cytoskeletal reorganization. SRC plays a crucial role in maintaining normal cell homeostasis and is involved in a wide range of physiological processes, including cell proliferation and survival, cytoskeleton regulation, cell shape control, intercellular contact maintenance, cell-matrix adhesion dynamics, motility, and migration. When activated in an oncogenic manner, SRC can stimulate increased cell growth and survival, contributing to tumor formation, while also promoting the actin cytoskeleton reorganization and reducing cell-cell and cell-matrix adhesion, which facilitates cell motility and invasion (Yeatman, 2004).

SRC contains an amino-terminal domain that is capable of myristoylation, an SH2 domain, an SH3 domain, a tyrosine kinase domain, and a negative regulatory element located at the

carboxy-terminus (Haura, 2006). SRC can undergo conformational changes that correspond to different activation states. In its inactive conformation, the phosphorylated C-terminal Tyr530 binds to the SH2 domain, while the SH3 domain stabilizes this state by interacting with the poly-proline motifs of the linker domain. This positioning brings both the SH2 and SH3 domains to the backside of the catalytic domain. When the intramolecular interactions mediated by the SH2 and SH3 domains are disrupted, SRC adopts an "open" active conformation, leading to phosphorylation of the activation loop at Tyr419 and subsequent activation (Guarino, 2010). SRC carries out its biological functions not only through its enzymatic activity but also due to its multi-domain structure, which enables it to interact with other proteins in key cellular compartments. Thanks to its amino-terminal fatty acid moiety, SRC associates with the plasma membrane and the perinuclear and endosomal membranes. In its inactive form, SRC is primarily localized in the juxtanuclear region. Upon stimulation, the SRC SH3 domain binds to actin filaments, driving SRC translocation to cell–cell and cell-matrix adhesion sites. There, it interacts with plasma membrane-bound molecular partners to participate in two major signaling events: signaling from receptor tyrosine kinases (RTKs), which mainly regulates cell growth, and signaling from adhesion receptors, including integrins and E-cadherin, which primarily control cytoskeleton functions (Bjorge et al., 2000). During cancer progression, SRC activity is often abnormally elevated. However, activating mutations or amplification of SRC are rarely observed in human tumors. Instead, an altered extrinsic regulation of SRC phosphorylation by kinases or phosphatases may play a crucial role in SRC upregulation. The inhibitory phosphorylation of Tyr530 is mediated by the kinase Csk, which acts as a major negative regulator of SRC. Protein tyrosine phosphatases (PTPs) are responsible for dephosphorylating either the C-terminal inhibitory site or the activation loop, thereby influencing SRC activity (Bjorge et al., 2000; Ingley, 2008).
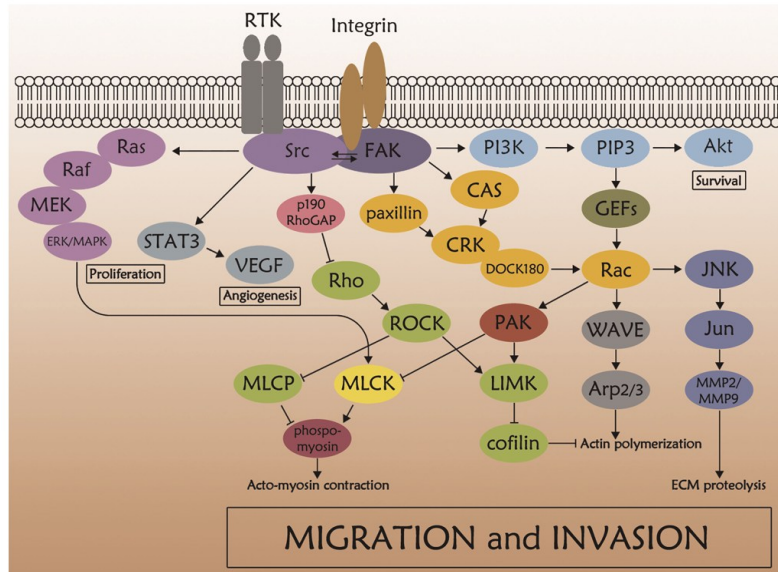
Figure 4. The main SRC-mediated transduction pathways which contribute to cancer progression
(Guarino, 2010)

Figure 4 shows all the substrate effectors of SRC. The tyrosine kinase FAK functions both as a signaling molecule and a scaffold that recruits SRC and its substrates to sites of integrin engagement. It plays a critical role in cell cycle progression, survival, adhesion, and migration (Berrier and Yamada, 2007). Integrin clustering leads to transient FAK dimerization, intermolecular autophosphorylation, and activation. Tyrosine phosphorylation of FAK creates a high-affinity binding site for the SH2 domain of SRC, recruiting and activating SRC. This results in the formation of a stable FAK-SRC complex, in which activated SRC phosphorylates FAK at multiple tyrosine residues. These additional phosphotyrosine sites further enhance the kinase activity of FAK (Playford and Schaller, 2004). The highly active FAK-SRC complex then promotes the phosphorylation of several FAK-associated SRC substrates, including CAS, paxillin, and p190RhoGAP, which are essential for actin cytoskeleton reorganization and migration (Playford and Schaller, 2004). At the leading edge of migrating cells, the FAK-SRC complex coordinates the assembly and disassembly of adhesions while promoting adhesion disruption at the rear. Notably, at the cell rear, the FAK-SRC complex recruits both ERK/MAPK and the protease calpain. This results in ERK/MAPK-induced activation of calpain, leading to proteolytic cleavage and disruption of adhesions, which enhances motility and invasion (McLean et al., 2005a) (Figure 5). At the leading edge, upon integrin ligation, SRC facilitates the phosphorylation of CAS, which recruits Crk. Crk then interacts with DOCK180, leading to the activation of Rac (Klemke et al., 1998). The latter plays a crucial role in cell migration by promoting the peripheral polymerization of actin beneath the plasma membrane, generating a pushing

force. Additionally, Rac can activate Jun N-terminal kinase (JNK), which triggers transcriptional activation and increases the expression of MMP-2 and MMP-9. So Rac promotes pericellular proteolysis and enhances cell invasion (McLean et al., 2005b). SRC stimulates the activation of Rac, which mediates the formation of membrane protrusions, and promotes the suppression of Rho by phosphorylating p190RhoGAP. p190RhoGAP facilitates the hydrolysis of active Rho-GTP to inactive Rho-GDP. This SRC-mediated suppression of Rho is crucial for alleviating contractile forces that would otherwise hinder protrusion at the cell front. Consequently, the integrin-mediated activation of SRC provides a mechanism to localize this suppressive pathway at the leading edge, enabling effective cell migration (Frame et al., 2002), whereas Rho function is prevalent rearward where it stimulates the assembly of acto-myosin fibres and the subsequent contractility (Guarino, 2010). Furthermore, at the cell front SRC promotes adhesion turnover by acting in concert with FAK, paxillin, and MLCK(Webb et al., 2004) (Figure 5).
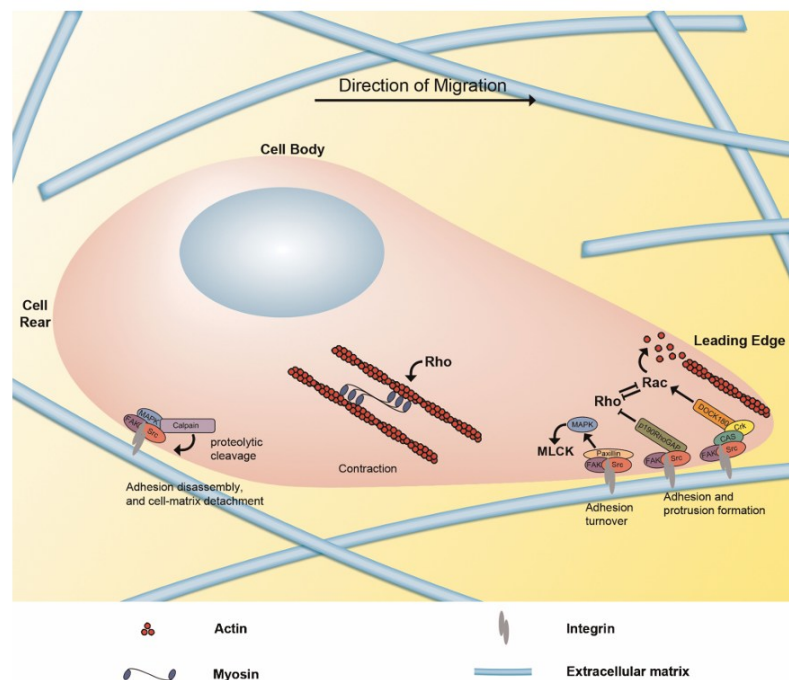

Figure 5. Role of SRC during cell migration

At the leading edge of a migrating cell, a cytoplasmic protrusion forms to establish new cell-matrix adhesions (right). This is followed by cytoskeletal contraction (center), which causes the cell body to slide forward, while previously formed adhesions behind the leading edge disassemble as the protrusion moves over them (adhesion turnover) (right). Finally, the cell rear detaches from the matrix and retracts into the advancing cell body (left), completing the cycle. Protrusive activity at the leading edge is driven by Rac-induced actin polymerization, while cell body contraction and retraction are mediated by Rho-dependent acto-myosin filaments. SRC regulates membrane protrusion by stimulating Rac and suppressing Rho, adhesion turnover in collaboration with FAK, paxillin, ERK, and MLCK, and the detachment of the cell rear from the matrix through calpain activation (Guarino, 2010)

1.3. KRIT1

KRIT1, also called CCM1, is a 736 amino-acid scaffold protein without defined catalytic domains while it contains several well-defined protein-protein interaction motifs and domains: a Nudix domain, three Asn-Pro-X-Tyr/Phe (NPx(Y/F)) motifs, an ankyrin repeat domain (ARD) and a FERM (band 4.1, ezrin, radixin, and moesin) domain (Su and Calderwood, 2020) (Figure 6).

KRIT1 signaling pathway has been extensively studied since mutations in its gene cause Cerebral Cavernous Malformations (CCMs), a rare familialr sporadic vascular disease (Retta et al., 2020). CCMs consists of closely clustered, abnormally dilated, and leaky sinusoidal capillaries (caverns) lined by a thin endothelium and devoid of normal vessel structural components, such as pericytes and astrocyte foot processes, which appear as multilobate "mulberry-like" vascular lesions on gross histopathological inspection. This condition results in the impairment of the blood–brain barrier that predisposes it to episodes of thrombosis and bleeding. Due to the cerebral haemorrhages, patients may present an increased risk for stroke, seizures, motor and sensory deficits, and non-specific headaches. However, many affected individuals are clinically asymptomatic during their entire life. These lesions are predominantly found in the central nervous system (CNS), including brain and spinal cord but are also known to affect retina, skin, and liver (Ercoli et al., 2020; Retta et al., 2020).

The molecular mechanisms at the basis of CCM pathogenesis linked to KRIT1 loss has not yet been completely defined, although KRIT1 ability to regulate several signaling pathways related to cell-cell interaction, cytoskeleton dynamics, angiogenic process, oxidative stress and inflammation has been demonstrated (Antognelli et al., 2018; Finetti et al., 2020; Goitre et al., 2017, 2014; Retta et al., 2020). Furthermore, KRIT1 have been shown to play an important role in mediating cell motility and migration, not only in endothelial cells but also in non-endothelial cells as cancer cells (Ercoli et al., 2020) and neutrophils (Nobiletti et al., 2023).
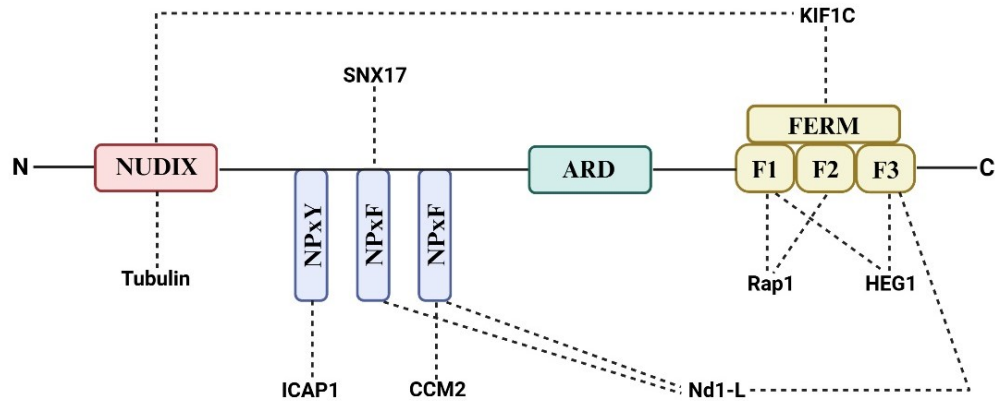
Figure 6. Schematic representation of KRIT1 protein
KRIT1 consists of a Nudix domain, three NPxY/F sites, an ankyrin repeat domain (ARD), and a FERM domain. FERM contains three subdomains (F1, F2, and F3). Dotted lines indicate intermolecular interactions that may occur through each protein domain

KRIT1 is ubiquitously expressed during early embryogenesis with pronounced endothelial expression in large vessels, followed by a restricted expression which persists up to adult life (Denier et al., 2002). During this second phase, KRIT1 is mainly expressed in endothelium and in neuronal cells of central and peripheral nervous system but is also present in various epithelia such as epidermal, digestive, respiratory, uterine, and urinary (Draheim et al., 2014; Ercoli et al., 2020).

KRIT1 has been observed in different cellular compartments, and it has been shown that its localization is controlled by the interaction with binding proteins. It is described that a polybasic sequence of KRIT1 within the Nudix domain is responsible for targeting to microtubules, while the interaction with Rap1 or HEG1 (Heart-of-Glass receptor) localizes the protein to cell membrane, and the formation of the KRIT1-ICAP1α complex is the driving force of the targeting to the nucleus. KRIT1 also interacts with SNX17 (a family member of the sorting nexin) at intracellular vesicles, and with Nd1-L which may contribute to nucleocytoplasmic shuttling of KRIT1 (Draheim et al., 2014; Fisher and Boggon, 2014; Guazzi et al., 2012).

In 1997 Serebriiskii et al. firstly identified KRIT1 as a Rap1 binding protein in a yeast two-hybrid screening (Serebriiskii et al., 1997). Rap1 is a member of the RAS family of GTPases that regulates cell–cell junctions in both endothelial and epithelial cells (Glading et al., 2007). The capacity of this protein to stabilize endothelial cell junctions depends on the interaction with KRIT1. Indeed, Rap1 regulates the junctional localization of the KRIT1 protein via FERM domain and increases the association of KRIT1 with junctional proteins such as β-catenin, vascular endothelial (VE)-cadherin, p120-catenin and AF-6 (also called afadin) (Glading et al., 2007). Consequently, KRIT1 depletion could induce the loss of a

stable cellular architecture and the activation of TGFβ/BMP signaling downstream of β-catenin (Ercoli et al., 2020). Another important binding partner of KRIT1 is ICAP1α (integrin cytoplasmic domain associated protein-1) which mainly works as a suppressor of β1 integrin. The interaction between KRIT1 and ICAP1α elicits the sequestration of ICAP1α from the membrane and consequently from the integrin tails, thus allowing the talin- and kindlin- mediated integrin activation (Fisher and Boggon, 2014). The members of the Kelch family proteins Nd1-L have been identified as a binding partner of KRIT1 in human endothelial cells. Nd1-L is localized in the nucleus, but it can interact with actin filaments and is involved in the regulation of cellular architecture, organization, and migration. The interaction between KRIT1 and Nd1-L occurs through the KRIT1 FERM and the second and third NPxY/F domains. This complex collaborates in the stability of the open conformation of KRIT1, necessary for its shuttle between nucleus and cytoplasm, and contribute to cellular protection from oxidative stress through the regulation of SOD2 enzyme expression (Guazzi et al., 2012).

Furthermore, KRIT1 loss in endothelial cells affects the intracellular redox homeostasis and results in increased reactive oxygen species (ROS) production through several distinct mechanisms, including Forkhead box protein O1 (FoxO1) and superoxide dismutase (SOD) downregulation, NOX4 upregulation and abnormal antioxidant responses (Antognelli et al., 2018; Goitre et al., 2012). In addition to the effects on endothelial cells, we recently showed that KRIT1 loss induces high levels of oxidative stress also in stromal cells through the upregulation of NOX1 (Finetti et al., 2020). Moreover, the increased intracellular ROS levels consequent to KRIT1 loss negatively regulate cell cycle by controlling FoxO-mediated downregulation of cyclin D1 and upregulation of p27Kip1 (Ercoli et al., 2020), and promote the production of proangiogenic factors, such VEGF and prostaglandin E2 (PGE2) (Goitre et al., 2012; Di Stefano et al., 2014; Finetti et al., 2020).

In endothelial cells, KRIT1 deficiency has also been shown to increase actin stress fibres and vascular permeability. KRIT1 is a negative regulator of RhoA and its effector ROCK. ROCK mediates actin stress fibres formation by increasing direct myosin light chain phosphorylation and by phosphorylating and inhibiting myosin phosphatase. As a result, cellular contractility is impaired. Pharmacological blockade of ROCK reversed KRIT1 depletion-induced MLC phosphorylation, actin stress fibres formation and endothelial monolayer permeability *in vitro*. *In vivo*, heterozygous Krit1+/- mice deficient in the encoded protein exhibited impaired pulmonary and cerebral vascular barrier function, which was reversed by treatment with the ROCK inhibitor fasudil. In addition, isolated

endothelium from various organs of Krit1+/- mice showed increased levels of phosphorylated MLC (pMLC) and actin stress fibres (Stockton et al., 2010).

In summary, it has been clearly demonstrated that KRIT1 is involved in different aspects of endothelial biology including vascular development, modulation of different redox-sensitive signaling and maintenance of endothelial barrier homeostasis, acting as an autocrine/paracrine factor (Finetti and Trabalzini, 2021).

1.3.1. KRIT1 in cancer

Since KRIT1 protein is involved in the regulation of numerous signaling pathways and is ubiquitously expressed, it is likely to be involved in other pathologies besides CCM, including cancer. However, few papers have been published so far that hypothesize a role of KRIT1 in tumor progression.

Glading and Ginsberg, with the intent to examine the effect of hemizygous KRIT1 deficiency on the development of β-catenin-driven cancers, generated Krit1+/− ApcMin/+ mice and demonstrated that the loss of one allele of KRIT1 induced more small intestinal adenomas in respect to Krit1+/+ ApcMin/+ mice and reduced their survival. They showed that KRIT1 loss caused β-catenin to dissociate from vascular endothelial (VE)-cadherin and to accumulate in the nucleus with consequent increase in β-catenin-dependent transcription, both *in vitro* and *in vivo* (Glading and Ginsberg, 2010).

Another evidence of the involvement of KRIT1 in cancer has been provided by Orso et al. They described an anti-correlation between the expression of KRIT1 and miR-21 in primary tumors. miR-21 is a well-known miRNA that displays oncogenic activity and is overexpressed in tumors. KRIT1 has been proposed as a target of miR-21 and appears to be able to counteract the pro-tumor functions of this miRNA in tumor cells (Orso et al., 2013). Ercoli et al. have described for the first time the involvement of KRIT1 in melanoma progression hypothesizing for this protein a role of tumor suppressor (Ercoli et al., 2020). It has been shown in melanoma human specimens that the downregulation of the expression of KRIT1 correlates with increased tumor aggressiveness. The idea that KRIT1 may act as a tumor suppressor has been investigated also in a melanoma cellular model in which KRIT1 loss increased the expression of β-catenin and its translocation into the cell nucleus, as described for intestinal tumorigenesis (Glading and Ginsberg, 2010). In this model the knockdown of KRIT1 induced up-regulation of N-cadherin and vimentin, that are involved in the epithelial mesenchymal transition (EMT)-associated protein network and in melanoma plasticity. In addition, expression levels of cyclooxygenase 2 (COX-2) and microsomal

prostaglandin E synthase 1 (m-PGES1) increased in KRIT1-knockdown cells in respect to control cells, pointing out the relevance of intrinsic inflammation in KRIT1 signaling and in melanoma progression. KRIT1 loss increased also melanoma cell growth, migration and invasion (Ercoli et al., 2020).

The involvement of KRIT1 in cancer has been also described by He et al. who showed that colon cancer cells regulate KRIT1 expression in endothelial cells by releasing exosomes. Exosomal miR-21-5p directly suppresses KRIT1 expression in the endothelium, thus promoting tumor angiogenesis and vascular permeability that fuel tumor progression (He et al., 2021). These observations outline the relevance of KRIT1-related signaling not only in tumor cells but also in stromal cells, that substantially contribute to tumor progression.

Contrary to previous works, Park et al. showed that increased KRIT1 expression is associated with increased metastasis in prostate cancer.

A significant increase of KRIT1 expression has been observed in samples of metastatic castration-resistant prostate cancer (mCRPC) compared with primary prostate tissues and other tumor stages. Consequently, an inverse correlation was also observed between the expression of KRIT1 with overall survival (OS) and metastasis-free survival. KRIT1 acts as a regulator of YAP/TAZ and AR signaling through the suppression of DDX5, which in turn regulates the suppression of YAP/TAZ. This signaling becomes hyperactive and drives prostate cancer progression with an unclear mechanism. In addition, in prostate malignancy the upregulation of KRIT1 is involved in the induction of the cadherin switch, an essential factor for tumor progression towards stages associated with greater aggressiveness (Park et al., 2021).

1.3.2. Nd1-L/NS1A

Nd1-L is a Kelch family member and represents the murine ortholog of the human Influenza virus NS1A-binding protein (Ivns1abp). The Kelch family proteins contain 4-7 Kelch motifs that form a propeller-like structure, and a BTB/POZ domain (broad complex, tramtrack and brick a brac/Pox virus and zinc finger) that mediates protein-protein interactions (Adams et al., 2000; Bardwell and Treisman, 1994).

The *Nd1* gene was originally isolated in murine cells and tissues as housekeeping gene coding a cytosolic, actin-binding protein involved in the dynamic organization of the actin cytoskeleton (Kang et al., 2001; Sasagawa et al., 2002).

Nd1-L was identified as a novel KRIT1 interacting partner by Guazzi et al. through yeast two-hybrid screening of a mouse embryo cDNA library. The interaction was then confirmed

by pull-down assays of recombinant proteins, as well as by co-immunoprecipitation of endogenous proteins in human endothelial cells (Guazzi et al., 2012). For the interaction between KRIT1 and Nd1-L the second and third NPXY/F motifs of KRIT are necessary but not sufficient. In fact, it cannot take place without an intact KRIT1 FERM domain, and some evidence indicate that the F3/PTB subdomain of KRIT1 is involved in the interaction. A bipartite model of interaction is thus assumed which is a molecular behaviour common to most FERM proteins, including KRIT1. This interaction helps maintain the open conformation of KRIT1 which is required for its shuttling between the nucleus and the cytoplasm for its function as a scaffolding protein. In addition, molecular assays showed that Nd1-L might support KRIT1 in regulating the expression levels of the ROS-scavenging enzyme SOD2, suggesting an important cooperation in cellular protection from oxidative stress (Guazzi et al., 2012).

Some Kelch proteins have been shown to play important roles in cancer. Overexpression of Nd1-L has been shown to suppress cancer cell metastasis and prolong the survival of tumour-bearing mice in an animal model. In addition, Nd1-L suppresses the activation of the Rho family GTPases RhoA, Rac and Cdc42, resulting in the suppression of invasion and migration of cancer cells. This observation strongly suggests that Rho family GTPases act downstream of Nd1-L. The reduction of Nd1-L in tumour cells can be considered one of the critical steps for the establishment of metastasis (Hatano, 2009).

The human homolog of Nd1-L, NS1A, plays an important role in organizing the dynamics of the actin cytoskeleton by stabilizing actin filaments through their association with F-actin via Kelch repeats. It protects against actin disruption and play a critical role in fundamental cellular functions such as cell division, cell movement and phagocytosis. These properties make NS1A an important regulator of cytoskeletal stability and therefore a potentially critical regulator of the macrophage phenotype. The *Ivns1abp* gene promoter is regulated by c-myc, which is modified by a variety of pathways downstream of inflammatory cytokines and is also involved in the induction of a large number of genes during alternative macrophage activation. Since the *Ivns1abp* gene plays an important role in both the coordination of actin cytoskeletal dynamics and cell shape, and since modifications of the macrophage cytoskeleton can regulate its pro-inflammatory state versus its pro-healing active state, the *Ivns1abp* gene is likely to play a role in the regulation of macrophage function (Hotter et al., 2020).

1.3.3. A new potential KRIT1 binding partner: KIF1C

The Kinesin superfamily (KIF) proteins share a highly conserved motor domain that enables motor binding and stepping across microtubules by converting the chemical energy of ATP hydrolysis into a mechanical force (Liu et al., 2013). The members of this superfamily participate in multiple normal cellular biological activities including mitosis and intracellular transport of vesicles and organelles. A number of KIF proteins have been found to be aberrantly expressed in a variety of cancer cells (Liu et al., 2013). KIF2C and KIF14 have been reported to be associated with progression of lung and breast cancers, KIF1C have been associated with brain metastasis and with cardiac myxoma (Grinberg-Rashi et al., 2009; Zhou et al., 2023). The small GTPase RhoB promotes membrane blebbing, thereby enhancing bleb-based amoeboid migration in cancer cells within 3D environments. The intracellular vesicular trafficking routes of RhoB play a key role in determining its localization and function. From the plasma membrane (PM), RhoB is internalized and transported via Rab5-positive early endosomes to either Rab7-positive late endosomes/lysosomes or Rab11-positive recycling endosomes. From recycling endosomes, RhoB can be redirected to the PM in a KIF13A-dependent manner. KIF13A is involved in anterograde trafficking, from the trans-Golgi network to the PM, and works together with Rab11 to support the transport and associated tubulation of recycling endosome membranes. The localization of RhoB at the PM is essential for its role in inducing membrane blebbing. KIF13A is required for RhoB-induced membrane blebbing and 3D amoeboid migration in leukemia cells. RhoB induces membrane blebbing through the well-characterized ROCK-Myosin II pathway (Gong et al., 2018).

In primary human macrophages KIF1C, a member of the Kinesin-3 family, is reported as a motor protein potentially involved in podosome regulation. The protein accumulations are in fact localized at microtubule plus ends and contacting regions of high podosome turnover. KIF1C interact also with nonmuscle myosin IIA, thus providing an interface between the actin and tubulin cytoskeletons (Efimova et al., 2014; Kopp et al., 2006).

In cancer cells KIF1C is localized at the tips of invadopodia and is required for invadopodia extension and cell invasion. Phosphorylation of tyrosine residues within the KIF1C stalk domain, induced by c-SRC, potentiates binding between KIF1C and microtubules by relieving autoinhibition. KIF1C could move along microtubules within invadopodia to deliver membrane lipids and proteins needed for their extension to their tips (Saji et al., 2022). KIF1C is also implicated in directional migration which requires the establishment and maintenance of long-term differences in structure and function between the front and

back of a cell. KIF1C is accumulated in trailing cell extensions and mediate the α5β1-integrins transport and accumulation to the tip of extensions. This activity is of crucial importance to allow structural maturation of trailing focal adhesion in response to contractile force and this, in turn, is crucial to maintain cell trails and coordinate rear retraction with the forward locomotion cells. In KIF1C absence, focal adhesions enlarge without increasing their adhesion protein content in response to contractile forces. Thus, focal adhesions are weaker while at the same time high forces build up at the rear of the cell. This will ultimately lead to loss of substrate contact and result in frequent and rapid retraction of cell tails and loss of cell polarity (Theisen et al., 2012).

KIF1C has been isolated by yeast two-hybrid screening of a mouse embryonic cDNA library as a potential interactor of KRIT1. The interaction was then confirmed by GST pull-down and co-immunoprecipitation assays of recombinant KRIT1 and KIF1C (Trabalzini et al., manuscript in preparation). This interaction further supports a possible role of KRIT1 in the regulation of mechanisms underlying cell invasion and migration processes.

2. AIM OF THE THESIS

KRIT1 is a scaffold protein involved in several cellular processes critical for tumor formation, including cell adhesion, cytoskeletal dynamics, and angiogenesis. It regulates cell adhesion by interacting with proteins like VE-cadherin and p120-catenin, which are essential for forming stable adherents junctions in endothelial cells (Glading et al., 2007). KRIT1 also influences cytoskeletal dynamics as an interactor of Nd1-L/NS1A, an F-actin stabilizing protein (Guazzi et al., 2012), and in endothelial cells, it serves as a negative regulator of RhoA and ROCK (Stockton et al., 2010). Furthermore, KRIT1 deficiency promotes the production of pro-angiogenic factors like VEGF and PGE2, mediated by the upregulation of NOX1 (Finetti et al., 2020). Disruption of these pathways in cancer cells can lead to enhanced invasion and metastasis.

In a previous work, we observed for the first time that the loss of KRIT1 is associated with increased tumour aggressiveness in human melanoma samples. KRIT1 depletion also resulted in enhanced β-catenin expression and its translocation to the nucleus, activating the Wnt/β-catenin pathway, and induced the expression of markers of inflammation, such as COX-2 and m-PGES1, and melanoma plasticity through the upregulation of mesenchymal markers, including N-cadherin and vimentin (Ercoli et al., 2020).

Moreover, we recently demonstrated that KRIT1 is able to interact with KIF1C (Trabalzini et al, manuscript in preparation). KIF1C is a kinesin family protein involved in the regulation of podosomes (Efimova et al., 2014; Kopp et al., 2006), and invadopodia (Saji et al., 2022), in directional migration, and in focal adhesion processes (Theisen et al., 2012).

Based on these findings, we hypothesize that KRIT1 may function as a tumor suppressor. The goal of this thesis is to investigate the potential role of KRIT1 in the acquisition of a malignant tumor phenotype, with a particular focus on invasion and migration processes.

To investigate this, the interactions between KIF1C, recently isolated by yeast two-hybrid screening, and NS1A, previously demonstrated for the murine homolog Nd1-L, were confirmed and studied in human tumor models. To explore the role of KRIT1 in the acquisition of an aggressive phenotype, migration and invasion were assessed following its depletion using both *in vitro* and *in vivo* assays. The link between KRIT1 loss and enhanced tumor aggressiveness was further examined by analysing the expression of this protein after treatment with pro-migratory stimuli. Additionally, the collaboration between KRIT1, KIF1C, and NS1A in promoting tumor plasticity was evaluated by analyzing stress fiber

formation and signaling pathways involving SRC, FAK, and RhoA/ROCK, which are known to play crucial roles in metastatic progression.

3. MATERIALS AND METHODS

3.1. Cell culture

HEK293 human embryonic kidney cells, A375 malignant melanoma cells, A549 lung carcinoma cells, AsPC1 pancreatic adenocarcinoma cells and PS1 pancreatic stellate cells (ATCC) were cultured in DMEM (Euroclone). Capan1 pancreatic adenocarcinoma cells and H2009 lung adenocarcinoma cells (ATCC) were cultured in DMEM F12 (Gibco). MRC5 lung fibroblast cells (ATCC) were cultured in EMEM (Sigma-Aldrich). H358 bronchioalveolar carcinoma cells and H441 lung papillary adenocarcinoma cells (ATCC) were cultured in RPMI 1640 (Gibco). All the media were supplemented with 10% fetal bovine serum (Euroclone), 100 U/ml penicillin/streptomycin (Euroclone), and 4 mM L-glutamine (Euroclone). H2009 medium was also supplemented with 0.005 mg/mL insulin, 0.01 mg/mL transferrin, 30nM sodium selenite, 10 nM hydrocortisone (Invitrogen),10 nM β-estradiol (Sigma-Aldrich), extra 2mM L-glutamine and 5% fetal bovine serum. The cells were grown at 37°C and 5% CO_2.

3.2. Plasmid and fusion proteins

Plasmids and fusion proteins used in the GST pull-down and ELISA experiments were prepared in a previous work (Guazzi et al., 2012; Trabalzini et al., manuscript in publication). The different GST-tagged proteins were expressed and purified by using the GST Gene Fusion System (GE Healthcare). Induction was performed by incubating transformed *E. coli* BL21 cells at 18–28 °C with IPTG (0.1–0.2 mM). GST fusion proteins were finally analyzed by Western blotting with anti-GST antibody (Amersham Bioscience). The amount of expressed proteins was determined by using the BCA method (Guazzi et al., 2012).

The MBP-tagged protein was expressed and purified by using the pMAL Protein Fusion and Purification System (New England BioLabs). Induction was performed by incubating transformed *E. coli* TB1 cells at 37 °C with IPTG (0.5 mM). MBP fusion proteins were finally analyzed by Western blotting with anti-MBP antibody (New England BioLabs). The amount of expressed proteins was determined by using the BCA method.

Full-length KRIT1A, KF1A (residues 418-736 of KRIT1A FERM domain) and K272NT (residues 1–272) were cloned as EcoRI/ SalI (Fermentas) inserts into pEGFP-C2 vector.

3.3. GST-Pull-down experiment

MBP fusion proteins (40 μg) (New England BioLabs) immobilized on 26 μL of amylose resin (75% in EtOH) were incubated for 1 h at room temperature with of HEK293 cells lysates overexpressing the GFP- tagged target proteins. The beads were subsequently washed three times with PBS buffer, added with SDS gel-loading buffer and finally analysed by SDS-PAGE followed by anti-GFP (Abcam) Western blotting.

3.4. ELISA format binding assay

100 μl of 'coating buffer' containing approximately 50 pmol of the three fragments GST-KRIT1A, GST-KNT272, GST-KFERM1A or GST was added to the wells of an ELISA plate (Nalgene Nunc International). After incubation at 4°C for 16 hours, the wells were washed twice with 100 μl of BSA 0.1% in PBS (w/v) (Sigma-Aldrich). Each well was incubated for 2 hours at 37°C with 100 μl of BSA 0.1% in PBS (w/v). At the end of the incubation, each well was washed twice with 100 μl of the same buffer used for saturation. Variable amounts (5-75 pmol) of MBP-KIF1C in 100 μl BSA 0.1% in PBS (w/v) were added to the wells. After incubation for 1 hour at 37°C, the wells were washed three times with 100 μl of Tween-20 0.1% in PBS (v/v). 100 μl of anti-MPB diluted 1:1000 in PBS was added to each well. Incubation was performed for 1 hour at room temperature. The wells were then washed three times with 100 μl Tween-20 0.1% in PBS (v/v). To each well, 100 μl of peroxidase-conjugated anti-rabbit IgG (Sigma-Aldrich) diluted 1:30.000 in PBS was added. After incubation for 1 hour at 37°C, the wells were washed three times with 100 μl of Tween-20 0.1% in PBS (v/v) and then spiked with 200 μl of TMB. The reaction was stopped after approximately 30 minutes by the addition of 100 μl of 0.5 M H_2SO_4.

The intensity of the staining in each well was determined by measuring the absorbance at 450 nm in an ELISA plate reader.

3.5. In silico analysis of KRIT1/KIF1C interaction

The KRIT1 and KIF1C primary structures were retrieved from UniProtKB reviewed (Swiss-Prot) database (The UniProt Consortium et al., 2023) with Entry code O00522 and O43896, respectively.

The KRIT1 and KIF1C primary structures were used as target sequences, and their 3D structures were generated through an AI algorithm named AlphaFold (Jumper et al., 2021). AlphaFold predicted 5 different 3D structures for each system using different weights and ranks them from best to worst by their mean predicted Local Distance Difference Test

(pLLDT) and the uncertainty metric ranges between 0 and 100, where 0 means high certainty and 100 means high uncertainty (lower is better). We selected the first model as best 3D structure generated by AlphaFold, showing mean pLDDT and uncertainty values of 83.72% and 3.5% for KRIT1 and 66.29% and 7.35% for KIF1C, suggesting a good overall quality of the 3D structures obtained.

To further optimize and relax the 3D structures for the docking simulation, a molecular modelling and energy minimization were performed using PyMOD3.0 with MODELLER 10.5 (Janson and Paiardini, 2021), using as template and target sequences the 3D structures generated by AlphaFold and the primary structures of KRIT1 and KIF1C, respectively. Lastly, the 3D structures were validated through PROCHECK analyses (Janson and Paiardini, 2021). CHARMM-GUI platform (Jo et al., 2008) was used to assign all molecular parameters for the energy minimization using charmm36-mar2019 force field, while GROMACS 2019.3 (Abraham et al., 2015) with CUDA Support was used to perform an energy minimization as suggested in a previous work (Trezza et al., 2024). In brief, the structure was immersed in a cubic box filled with TIP3P water molecules and counter ions to neutralize the net charge of the system. Simulation was run applying periodic boundary conditions. The energy of the system was minimized with 5.000 steps using the steepest descent algorithm to converge to a minimum energy with forces less than 100 kJ/mol/nm. The equilibration was performed integrating each time step of 2 fs; a V-rescale thermostat maintained the temperature at 300 K and Noose-Hoover barostat maintained the system pressure at 1 atm, with a low dumping of 1 ps−1; the LINCS algorithm constrained the bond lengths involving hydrogen atoms. The 3D structures of KRIT1 and KIF1C were extracted and used as starting structure for the docking simulation.

Protein-protein interaction between KRIT1 and KIF1C was predicted by GRAMMX tool (Tovchigrechko and Vakser, 2006). In detail, the free docking was choose as docking methodology selecting 10 number of top matches to output as PDB files. The docking parameters were set choosing 60000 as number of scans matches to output enabling the clustering of docking poses. The number of top predictions to perform clustering and the clustering threshold (RMSD < A) were set to 60000 and 6A, respectively. Based on a previous work, we added in the "interface residue constrains" section the KRIT1 FERM domain residues (420-734) as "active" residues (potentially involved in the interaction), all other residues were defined as "passive" (potentially not involved in the interaction).

The first binding pose was selected as best docking pose and PDBePISA tool (Krissinel, 2010) revealed the binding residues mostly involved in polar interactions between KRIT1

(458,459,462,513,631,632,684,685,698,703,723,724,731,732,734,735,736) and KIF1C (21,22,24,254,257,258,259,264,504,505,506,527,638,640,641,643,644,651,652,658,740), thus, a rational docking was performed using the same parameters previously described adding as "active" residues the residues involved in the polar interaction network.

3.6. Co-immunoprecipitation assay

A375 and A549 were seeded (1.0 x 10^6 cells/well) in Petri dish 100 mm with DMEM with 10% FBS. After 48 h, cells were lysed and centrifuged at 13.000 × g for 15 min at 4 °C. Protein content was measured using a BCA protein assay kit (Thermo Scientific). For co-immunoprecipitation, aliquots of cell extract supernatants containing an equal amount of proteins (100 µg) were analysed. 25 µL (0.25 mg) of magnetic beads (Thermo Scientific) were combined with the protein extract. The reaction volume was adjusted to 150 µL with Ripa Buffer (Cell Signaling Technology). The reaction was maintained for 1 hour at 4°C while mixing. After, the supernatant was combined with 1 µg of antibody (anti-KRIT1, anti-KIF1C, or anti-NS1A) and incubated overnight at 4°C with mixing. The day after the antigen/sample mixture was added with 25 µL (0.25 mg) of pre-cleaned magnetic beads and incubated at room temperature for 1 h with mixing. After washing, 25 µL of 0.1 M glycine pH 2.0 was added and incubated for 10 min at room temperature with mixing. The beads were magnetically separates and the supernatant containing target antigen was recovered. 25 µL of neutralization buffer, Tris 1M pH 7.5-9, and Laemmli buffer were added to perform Western blot analysis.

3.7. Immunofluorescence

A375 and A549 cells (5.0 x 10^4 cells/well) were seeded on glass coverslips. After 24 h cells were fixed with cold acetone (KRIT1 and KIF1C staining) for 5 min in ice or with PFA (Thermo Scientific) at 4% for 20 min (NS1A staining). Cells fixed with PFA were subsequently permeabilized with 0.1% triton BSA for 10 min and then were incubated with 3% BSA for 1 h and stained overnight at 4 °C with primary antibody for KRIT1 (1:100, Abcam), KIF1C (1:300, Abcam), NS1A (1:300, Abcam), β-Tubulin (1:300, Santa Cruz) or pFAK (1:200, Cell Signaling Technology). Slips were washed three times with 0.5% BSA and then incubated 1 h at room temperature with secondary antibodies Alexa Fluor Rabbit 488 (1:500, Invitrogen), Alexa Fluor Mouse 555 (1:500, Cell Signaling Technology), Alexa Fluor Mouse 488 (1:2000, Invitrogen) or Alexa Fluor Rabbit 555 (1:1000, Cell Signaling Technology). Alternatively, slips were incubated with Phalloidin-488 for 15 min (1:20, Cell

Signaling Technology). Microscopy imaging was performed on a Zeiss LSM700 confocal microscope using a 60X objective. Colocalization analyses were carried out on three different sections for each cell using ImageJ and the JACoP plugin to calculate Manders' coefficient M1. This coefficient indicates the proportion of the green signal coincident with a signal in the red channel over its total intensity. Manders' coefficients range from 0 to 1, corresponding to non-overlapping images and 100% colocalization between both images, respectively.

3.8. siRNAs transfection

A375 and A549 cells, were plated (2.5×10^5 cells/well) in 6 well multiplate and after adhesion transfected with 10 nM of negative control, KRIT1 siRNA, KIF1C siRNA, NS1A siRNA (Qiagen) using 5 µL of lipofectamine 3000 (Invitrogen) according to manufacturer's instructions. 24 h post-transfection, media was changed. Cells were lysed 48 (KIF1C, NS1A siRNAs) and 72 h post-transfection (KRIT1 siRNA) and further analyzed by Western blotting.

3.9. Xenograft in zebrafish embryos

A375 cells (1.5×10^5) were transfected with siRNA. After 48 h, cells were harvested using trypsin, counted, centrifuged (5 min, 300 x g) and washed once with PBS. Then, cells were resuspended in 5 mL of PBS solution containing 5 µL of C7001 Cell Dye 1 mg/mL (Invitrogen) and incubated 15 min at 37°C and then 15 min at 4°C. Stained cells were centrifuged again (5 min, 300 x g) and were resuspended with 1 mL of PBS. Cell suspensions were transferred in a 1.5 mL tube and subjected to an additional centrifugation step (5 min, 300 x g). PBS was completely removed, and the tube was cooled down on ice. Cells were washed once in FBS and then in PBS. Cells were finally resuspended with PBS at the final concentration of 5 µL per 1×10^6 cells.

Concurrently to cell staining procedures, 48 hpf (hours post fertilization) zebrafish embryos of the Casper and the Tg (kdrl: EGFP) were dechorionated manually by forceps (Dumont No. 5, #F6521-1EA, Sigma-Aldrich) and anesthetized with 0.17 mg/mL tricaine (Sigma-Aldrich, A5040). Cell suspension was loaded into a borosilicate glass capillary and 1 nL (200 cells for migration) were injected into the yolk sac of the dechorionated embryos, using a microinjector (Tritech Research). Then, embryos were incubated at 36°C for 96 h. At least 80 embryos were injected per experimental condition and each experiment was repeated three times. At the end of treatment period, fluorescence imaging was carried out using the

Leica MZ10F Stereomicroscope equipped with DFC3000 G camera and Leica Application Suite X. Pictures were taken after microinjection and after 96 h of treatment. The migration was positive if the cancer cells reached the tail of the fish and negative if they remained confined to the yolk sac. Data were analysed using Fisher test.

3.10. Stimulation of cells with PMA

A375 and A549 cells were seeded (2.5×10^5) in 60 mm Petri dishes and grown at 37°C and 5% CO_2. After 24 h, cells were starved for another 24 h with fresh medium 0.1% FBS. Cells were then treated with 2% FBS and 80 ng/mL PMA and lysed 48 h post treatment. Cell lysates were further analyzed by Western blotting.

3.11. Western Blotting analysis

Cells lysates were centrifuged at 13.000 × g for 15 min at 4 °C. Protein content was measured using a BCA protein assay kit (Thermo Scientific). For Western blotting analysis, aliquots of cell extract supernatants containing an equal number of proteins (50 μg) were treated with Laemmli buffer (Biorad), boiled for 5 min, resolved on 10-20 % stain-free gel (Biorad) and then blotted onto a nitrocellulose membrane (Biorad). Membranes were incubated overnight with the following primary antibodies: anti-KRIT1 (1:1000, Abcam), anti-KIF1C (1:1000, Abcam), anti-phospho-KIF1C (1:1000, Invitrogen), anti-NS1A (1:3000, Abcam), anti-ROCK (1:1000, Cell Signaling Technology), anti-RhoA (1:1000, Cell Signaling Technology), anti-RhoC (1:1000, Cell Signaling Technology), anti-pSRC (1:1000, Cell Signaling Technology), anti-SRC (1:1000, Cell Signaling Technology) or anti-GAPDH (1:1000, Cell Signaling Technology). The membranes were then incubated with 1:3000 dilutions of horseradish peroxidase-conjugated secondary antibody (Cell Signaling Technology) for 1 h at RT. Chemiluminescence was detected by Image Quant Las 4000 imager (GE Healthcare). Data were analysed with Image J software and statistical analysis was made with T-test. Results were expressed as arbitrary densitometry unit (A.D.U.).

3.12. Scratch assay

A375 and A549 cells were seeded (3.0×10^5 cells/well) in 24-well multiplate in DMEM 10% FBS. After 24 h, cell monolayers were scored vertically down the middle of each well with a sterile tip. Each well was washed with PBS to remove detached cells. Cells were treated with 2% FBS and with PMA (ChemCruz) at the final concentration of 80 ng/mL. Images of the wound in each well were acquired at time 0 and after 24 h with 10X magnification

(Nikon, Eclipse Ts2). Images were analysed with Image J and results were expressed as arbitrary units of wound and percentage of healing taking as reference the area at time 0. Statistical analysis was made with T-test.

3.13. Hanging Drop Spheroid

H358, H441, H2009, Capan1 and AsPC1 were seeded (2.5 x 10^5 cell/well) in 6-well multiplate in corresponding medium 10 % FBS. After 24 h cells were transfected with the siRNA. After another 24 h, hanging droplets were seeded. Each droplet was 20 µL and consisted of methylcellulose and a cell volume containing 4.4 x 10^4 cancer cells (H358, H441 and H2009) plus 2.2 x 10^4 fibroblast cells (MRC5) or 2.2 x 10^4 cancer cells (Capan1 and AsPC1) plus 4.4 x 10^4 fibroblast cells (PS1). The day after spheroids were harvested in the organotypic gels made by high concentration collagen (final concentration 2 mg/mL) (Corning), Matrigel (175 µL) (Corning), Hepes (1M, pH 7.4, 25 µL), NaOH (1N, 10 µL) and media up to 1 mL.

Images of each spheroid were acquired after 8 days (H358 and H441) or 5 days (H2009, Capan1, AsPC1) days after siRNA treatment with 10X magnification (Zeiss, Axiovert 135). Images were analysed using Image J and statistics were performed using T-test.

4. RESULTS AND DISCUSSION

4.1. KIF1C is a novel KRIT1 binding partner

KRIT1 contains domains and motifs that mediate binding to other proteins and lacks functional enzymatic activity or nucleotide binding regions. The presence of these domains, as well as KRIT1 known molecular interactions, strongly indicate that this protein can act as a scaffold for the assembly of functional protein complexes involved in physiologically important signaling networks and suggests that the identification of novel molecular interactors may represent a crucial step in elucidating its function.

To identify new binding partners of KRIT1, a yeast two-hybrid screening of a mouse embryo cDNA library has been recently performed using as bait the fragment of KRIT1 cDNA encoding the FERM domain. This screening allowed the isolation of KIF1C, a kinesin superfamily member, as a potential interactor of KRIT1. The KRIT1/KIF1C interaction initially isolated by two-hybrid screening was then confirmed by pull-down and co-immunoprecipitation assays of recombinant proteins, as well as by co-immunoprecipitation of endogenous proteins in human endothelial cells (Trabalzini et al. manuscript in preparation).

To further characterize the newly isolated interaction and map the regions of KRIT1 involved in the binding to KIF1C, in this work a GST pull-down assay of whole-cell extracts from HEK293 cells overexpressing GFP-KF1A (KRIT1A FERM domain, residues 418-736), GFP-KNT272 (residues 1-272 of KRIT1) or GFP-K1Afull (full-length KRIT1A) was performed using MBP-KIF1C (556-713) fusion protein as a bait. Bound fractions were then subjected to Western blot analysis with an anti-GFP antibody. As expected, both the C-terminal fragment of KRIT1 containing the FERM domain and full-length KRIT1 were able to interact with KIF1C, and in addition, also the N-terminal fragment of KRIT1 interacted with KIF1C (Figure 7). These results suggest that both the N-terminal region of KRIT1 and the FERM domain are involved in the interaction with KIF1C.
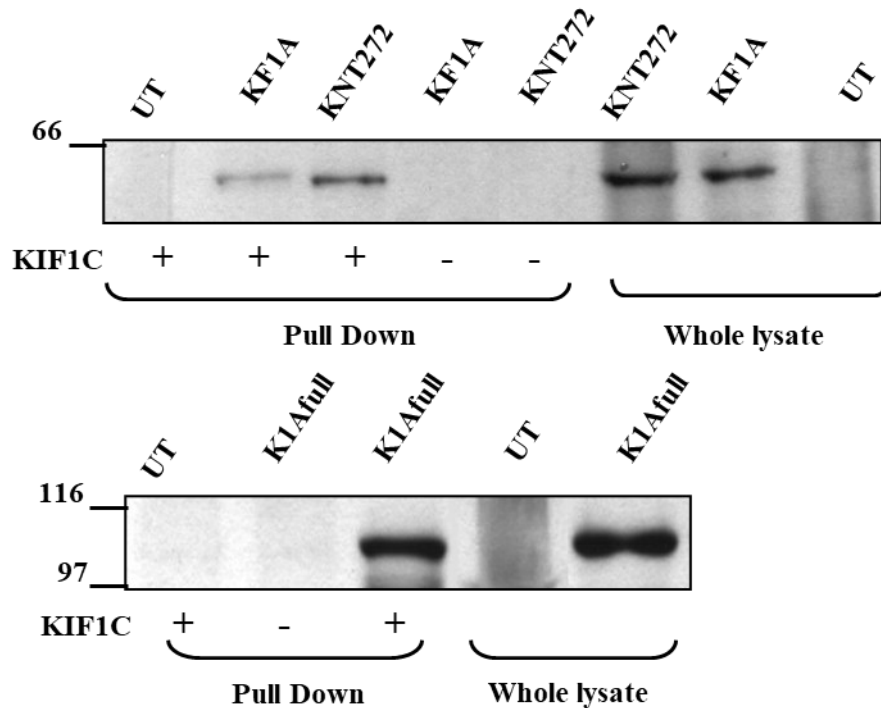
Figure 7. The KIF1C polypeptide binds to KRIT1 protein in a pull-down assay
HEK293 cells were transiently transfected with a pEGFP vector containing K1Afull, KNT272, or KF1A. The pull-down assay was performed by incubating cell lysates with MBP-KIFC (556-713) immobilized on amylose-resin, as indicated. Incubation of MBP-KIF1C (556-713) with untransfected cell lysates and incubation of transfected cells with the amylose-resin were used as negative controls.
The different incubation mixtures were then analyzed by SDS-PAGE and Western blotting with GFP antibody together with transfected and untransfected whole cell lysates.
UT: untransfected cells
KNT272: residues 1-272 of KRIT1
KF1A: KRIT1A FERM domain (residues 418-736)
K1Afull: KRIT1A full length

To confirm the results obtained with the GST pull-down, and to perform a quantitative assessment of the interaction between the two different regions of KRIT1 and KIF1C, an *in vitro* ELISA binding assay has been subsequently carried out. The results obtained confirmed that both full-length KRIT1 and the two N- and C-terminal fragments of KRIT1 interact with KIF1C, but not with the same affinity (Figure 8). In particular, the extent of binding of the full-length protein (green curve) is greater than that of the partial fragments; furthermore, KRIT1A FERM domain (yellow curve) interacts with KIF1C with greater affinity than KNT272 (pink curve). This data further supports the hypothesis that two distinct regions of KRIT1 are required for the interaction with KIF1C (Figure 8), as demonstrated by Guazzi et al. for the interaction between KRIT1 and Nd1-L (Guazzi et al., 2012).
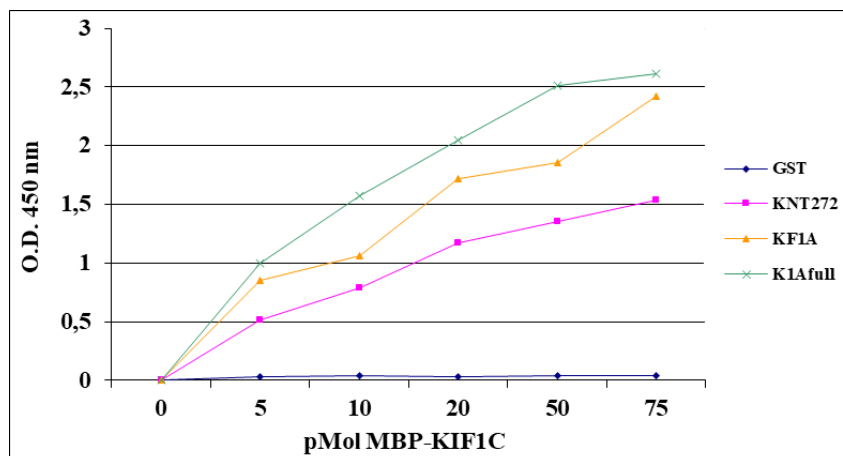
Figure 8. Analysis of the KRIT1/KIF1C interaction by ELISA format binding assay
Binding curves were generated by serially varying the concentration of MBP-KIF1C (556-713) while maintaining the amount of the different fragments of GST-KNT272, GST-KF1A, K1Afull at 50 pmol/well. Recombinant GST was used in a negative control assay and determined the background binding of the assay. Protein-protein interaction was detected by using anti-MBP antibody. Absorbance values are plotted as a function of the test protein concentration. The data shown are representative of three separate assays performed in triplicate.
KNT272: residues 1-272 of KRIT1
KF1A: KRIT1A FERM domain (residues 418-736)
K1Afull: KRIT1A full length

The 272 aa N-terminal fragment of KRIT1 contains a NPXY motif required for KRIT1 interaction with ICAP1 (Zawistowski et al., 2002; Zhang, 2001) and two additional NPXY/F motifs required for the interaction with CCM2 (Zawistowski et al., 2005; Zhang et al., 2007). In addition, the region containing the second and third NPXY/F motifs has been demonstrated to be involved in the intramolecular interaction with the PTB-like subdomain of the C-terminal FERM domain, playing a pivotal regulatory role in the control of the KRIT1A open/closed conformation switch (Francalanci et al., 2009). The results of both pull-down and ELISA binding assay indicate that also this region of KRIT1 is involved in the interaction with KIF1C, suggesting a bipartite interaction model which is reminiscent of the well characterized bipartite interaction between the FERM domain-containing adaptor protein Talin and integrin β-subunit cytoplasmic tails (Gingras et al., 2009; Goult et al., 2009), which plays a major role in regulating integrin affinity for extracellular ligands (Calderwood, 2004; Calderwood et al., 2004) and coupling to the actin cytoskeleton (Critchley and Gingras, 2008; Ziegler et al., 2008). Indeed, both the N-terminal FERM and the C-terminal rod domains of Talin have been found to interact with the cytoplasmic tail of integrin β-subunits. Interestingly, Talin may also undergo an autoinhibitory intramolecular interaction involving its N- and C-terminal portions whereby binding sites for interactors are masked. Remarkably, this molecular behaviour is common to most FERM proteins, including KRIT1 (Francalanci et al., 2009). Taken together with these analogies, our results

33

point to a model where both the N- and C-terminal portions of KRIT1 are involved in the molecular interaction with KIF1C, which in turn may contribute to maintaining the KRIT1 open conformation required for its functioning as a scaffolding protein (Francalanci et al., 2009).

To confirm *in vitro* results and to identify the potential amino acid residues critical to the KRIT1/KIF1C binding, the molecular patch interacting between two proteins was dissected. GRAMMX software performed and provided the potential KRIT1-KIF1C binding pose. Interestingly, the docking simulation predicted two main docking pose clusters, the first one showed the interaction of KIF1C exclusively on the KRIT1 FERM domain with an energy of interaction of -800 kJ/mol (Figure 9A), while the second one exhibited the KIF1C interaction involving both the FERM domain and N-terminal of KRIT1 with an energy interaction of -723 kJ/mol (Figure 9B).

The similarity of binding energies between the interaction involving a single portion of KRIT1 and that involving two portions does not allow for greater certainty in predicting which of the two occurs.

In addition, as the information on the three-dimensional structure of full-length KIF1C is currently incomplete, molecular dynamics analysis of the interaction KRIT1/KIF1C could not be performed.

Consequently, to discriminate the potential KIF1C binding pose on KRIT1, *in silico* results were based on the previous study by Guazzi et al. showing that the interaction KRIT1/Nd1-L involves both the FERM and the N-terminal domain of KRIT1 (Guazzi et al., 2012), and on the indications deriving from the pull-down and ELISA assays reported above (Figures 7 and 8). Thus, the binding pose of KIF1C able to trig interactions with the C- and N -terminal domains of KRIT1 was selected for further *in silico* analyses.
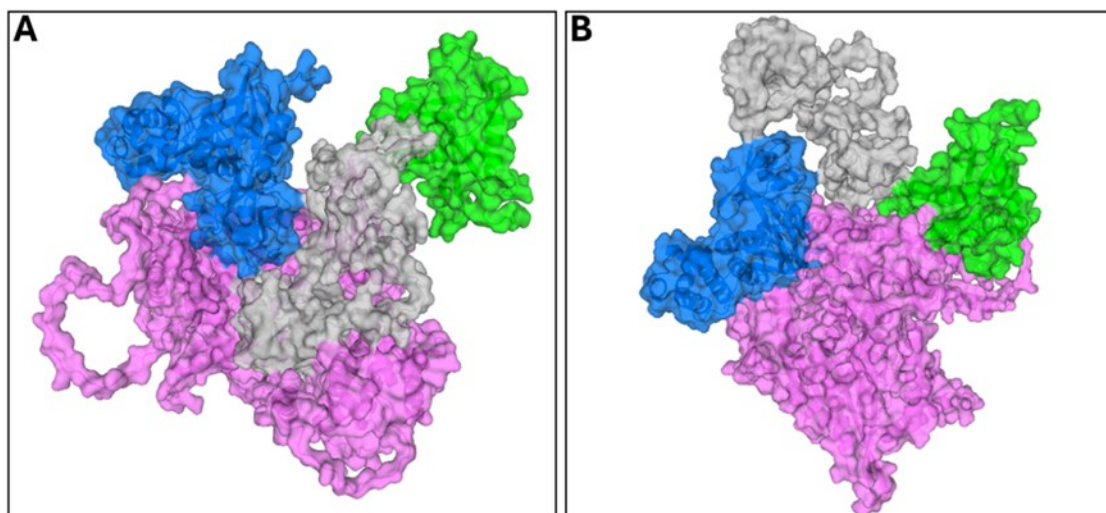
Figure 9. Docking simulation of the interaction between KRIT1 and KIF1C
Two potential interactions were identified: (A) KIF1C interacts exclusively with the KRIT1 FERM domain.
(B) KIF1C interacts with both KRIT1 FERM and N-terminal domains.
KRIT1 is represented in green (N-terminal domain), in grey (ankyrin repeat domain), in blue (FERM domain), KIF1C is represented in pink

PDBePISA explored and defined the interaction network of the complex, showing a very large patch of hydrophobic and strong polar interactions (Table 1) involving the KRIT1 C- and N-terminal domains, confirming the experimental evidence of the KRIT1 molecular interactor binding region.

KRIT1 (Binding residue)	KIF1C (Binding residue)	Distance (Å)	Bond type
Arg- 29 (NH2)	Ile-539 (O)	3.75	H-bond
Arg-734 (NH1)	Glu-506 (OE2)	3.85	H-bond
Arg-734 (O)	Asn-505 (ND2)	2.92	H-bond
Asn-735 (N)	Asn-505 (OD1)	3.74	H-bond
Asp-137 (OD1)	Gln-542 (NE2)	3.54	H-bond
Cys-685 (N)	Ser-257 (O)	2.99	H-bond
Gln-136 (OE1)	Gln-542 (N)	3.65	H-bond
Gln-458 (NE2)	Asp-638 (OD2)	3.83	H-bond
Gln-459 (OE1)	Leu-641 (N)	3.40	H-bond
Gln-689 (OE1)	Lys-658 (NZ)	2.84	H-bond
Glu-223 (O)	Asn-652 (ND2)	3.46	H-bond
Glu-631 (N)	Ser-21 (O)	2.95	H-bond

Glu-631 (O)	Ala-24 (N)	3.85	H-bond
Glu-703 (O)	Arg-254 (NH1)	3.16	H-bond
Gly-684 (O)	Gly-259 (N)	2.81	H-bond
Gly-684 (O)	Ser-258 (N)	3.13	H-bond
Ile-632 (N)	Gln-22 (O)	2.63	H-bond
Lys- 31 (NZ)	Gln-527 (OE1)	3.39	H-bond
Lys-724 (NZ)	Met-643 (O)	3.84	H-bond
Met-723 (N)	Glu-651 (OE1)	3.67	H-bond
Pro-731 (O)	Arg-264 (NH1)	3.67	H-bond
Ser-736 (OG)	Leu-504 (N)	3.66	H-bond
Thr-20 (O)	Arg-740 (NH1)	2.54	H-bond
Thr-462 (OG1)	Glu-644 (OE1)	3.54	H-bond
Thr-462 (OG1)	Lys-640 (NZ)	3.36	H-bond
Thr-732 (OG1)	Arg-264 (NH2)	2.48	H-bond
Arg-513 (NE)	Glu-644 (OE2)	3.97	Salt Bridge
Arg-513 (NE)	Glu-644 (OE1)	3.03	Salt Bridge
Arg-513 (NH1)	Glu-644 (OE1)	3.44	Salt Bridge
Arg-513 (NH2)	Glu-644 (OE2)	2.85	Salt Bridge
Arg-734 (NE)	Glu-506 (OE2)	3.64	Salt Bridge
Arg-734 (NH1)	Glu-506 (OE2)	3.85	Salt Bridge
Lys-31 (NZ)	Glu-541 (OE1)	3.00	Salt Bridge

Table 1. KRIT1/KIF1C binding residues
In round brackets are reported the atom types (HB-SB-donor/acceptor) of residues involved in H-Bond and Salt Bridges interactions (the hydrophobic interactions are not shown)

However, data obtained through yeast two-hybrid screening, GST pull-down and ELISA binding assay suggest a bimodal interaction.

The *in silico* analysis, combined with data obtained from the *in vitro* binding assays and previous results, suggest a bimodal interaction and a strong involvement of the FERM domain in the interaction between KRIT1 and KIF1C. Indeed, this domain has been found to be implicated in all the binding poses between KRIT1 and KIF1C that were generated, and it displays a comparable profile in its interaction with Nd1-L. Furthermore, molecular dynamics analysis of the interaction KRIT1/Nd1-L demonstrated that binding initiates with the N-terminal portion of KRIT1, followed by a structural rearrangement, and culminates in

binding to FERM, which effectively blocks the interaction between the proteins (Trabalzini et al. unpublished data).

4.2. KRIT1 interacts with KIF1C and NS1A in cancer cells

Several pieces of evidence suggest that KRIT1 may play a role in cancer onset and progression, acting as a tumor suppressor by regulating mechanisms underlying cell migration and invasion. The two recently identified KRIT1 binding partners, Nd1-L and KIF1C - both involved in the regulation of cytoskeleton dynamics and rearrangements associated with cell movement and cancer progression - could mediate this function.

In this work we investigated the significance of these two KRIT1 molecular interactions in human cancer; therefore, we used two different human cancer cell lines, A375 (melanoma cancer cells) and A549 (lung adenocarcinoma cells), and focused on human KIF1C and NS1A protein, the human orthologue of Nd1-L.

To confirm the interaction of KRIT1 with KIF1C and NS1A in cancer cells, co-IP of endogenous KRIT1 and either KIF1C or NS1A in both cancer cell models was performed. As shown in Figure 10A, endogenous KIF1C and NS1A co-immunoprecipitated from A375 and A549 cell lysates probed with an anti-KRIT1 antibody. KRIT1 was consistently detected when co-immunoprecipitation was performed using either KIF1C or NS1A antibodies (Figure 10B and C). These data clearly demonstrate that the KRIT1/KIF1C and KRIT1/NS1A interaction occurs in cancer cell lines.
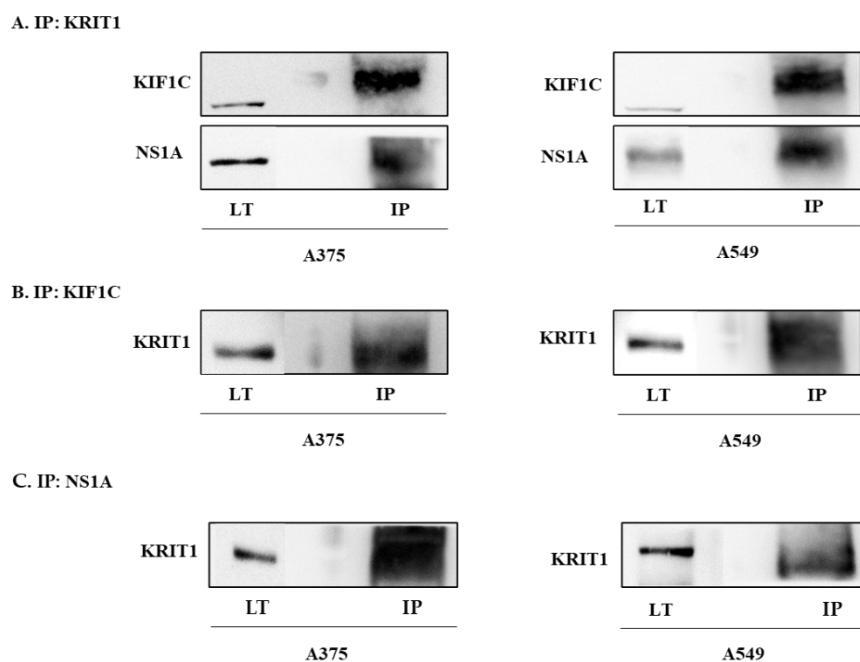
Figure 10. Both KIF1C and NS1A co-immunoprecipitate with KRIT1 in cancer cells
Lysates from A375 and A549 cells were immunoprecipitated with anti-KRIT1 (A), anti-KIF1C (B) and anti-NS1A (C) antibodies, and then analyzed by SDS-PAGE and Western blotting with anti-KIF1C and anti-NS1A (A), anti-KRIT1 (B and C) antibodies. An aliquot of the A375 and A549 cells lysate was loaded in the same gel as positive control for the immunodetection phase
LT: Total lysate
IP: Co-immunoprecipitate

All KRIT1, KIF1C and NS1A have been reported to be associated with the cytoskeleton. It has been established that KRIT1 associates with microtubules to form a complex with β-tubulin (Gunel et al., 2002). A direct interaction between actin and the Kelch repeats of Nd1-L has been described, protecting cells from stress induced by actin depolymerization (Kang et al., 2001; Sasagawa et al., 2002). It has also been reported that KIF1C binds to non-muscle myosin IIA via its PTPD-binding domain, providing an interface between the actin and tubulin cytoskeletons (Kopp et al., 2006).

To prove the link between KRIT1, KIF1C and NS1A with the cytoskeleton and cellular dynamics, immunofluorescence was performed to study cellular localization of the three proteins. In Figure 11 it is shown that not only KRIT1 but also KIF1C and NS1A colocalize with β-tubulin.
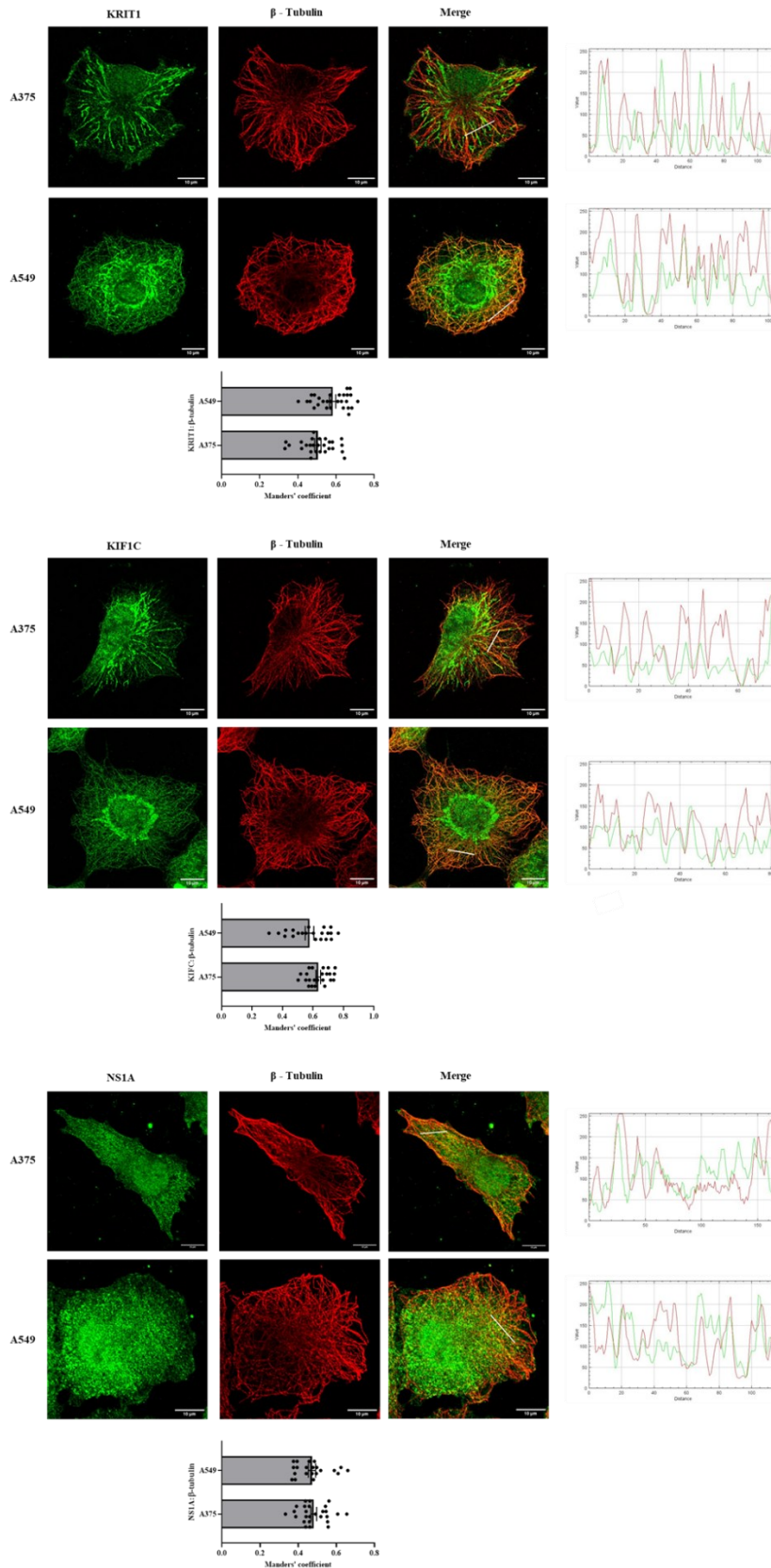
Figure 11. Co- localization of KRIT1, KIF1C and NS1A with β-tubulin in cancer cells
Immunofluorescence analysis of A375 and A549 cells co-stained for (A) KRIT1, (B) KIF1C and (C) NS1A
(green) and β-tubulin (red). Right, intensity profiles along the white lines within the selected area in the
overlay images for each channel are shown. Below quantification (mean ± SEM) using Manders' coefficient
of colocalization of each protein with β-tubulin (10 cells/sample, n≥3)

4.3. KRIT1 is involved in cancer cell migration and plasticity

It has been recently demonstrated that KRIT1 knockdown in human melanoma cells promotes *in vitro* migration and invasion (Ercoli et al., 2020).

To study the molecular mechanisms associated with KRIT1 downregulation and cancer cell migration, we evaluated the effects of generic chemotactic stimuli such as FBS and phorbol myristate acetate (PMA) on A375 and A549 cell lines using a scratch assay. Both treatments significantly induced cell migration after 24 h of incubation (Figure 12A), which was accompanied by a simultaneous reduction in KRIT1 expression (Figure 12B).
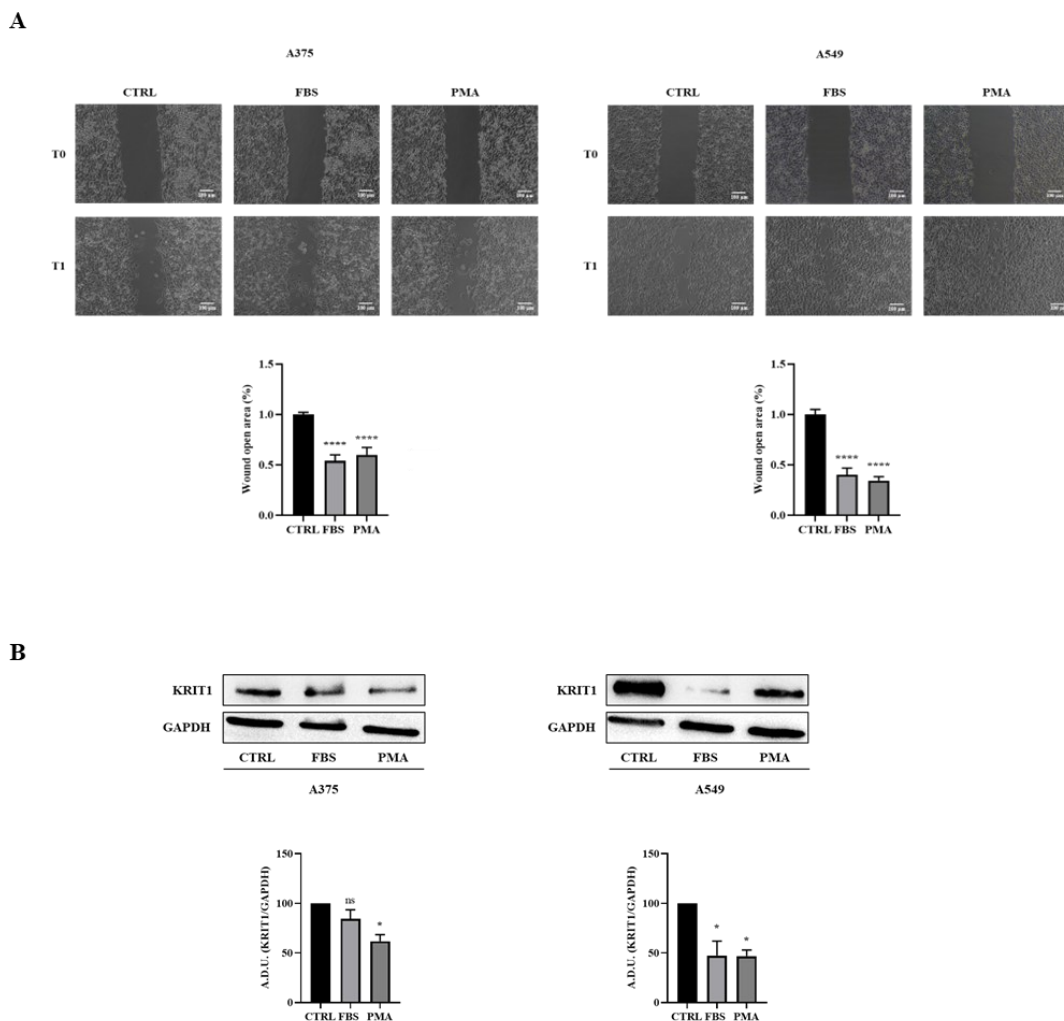

Figure 12. Cells treated with pro-migratory stimuli exhibit a reduction in KRIT1 expression
(A) Confluent monolayers of A375 and A549 cells were scratched and treated with FBS (2%) and PMA (80 ng/mL). Images were taken for 24 h post-wounding at 10X magnification. Data is reported as a percentage of wound open area for well and are representative of three independent experiments
(B) A375 and A549 cells were treated with FBS (2%) and PMA (80 ng/mL) for 48 h. Images are representative of three independent experiments
*p<0,05; ****p<0,0001

Thus, increased cell migration is associated with KRIT1 downregulation in cancer cells.

To further confirm this observation in *in vivo* models we investigated whether A375 knockdown for KRIT1 with a hypothetical high metastatic potential, could disseminate throughout the zebrafish body. SiCTRL and siKRIT1 A375 cells were injected into the yolk sac of 48 h post fertilization embryos and analysed at 96 h post injection using stereomicroscope, where a significant spread of cancer cells could be seen throughout the tail of the fish (Figure 13). These data indicate that KRIT1 loss confers metastatic potential to cancer cells, prompting the search for the molecular mechanisms underlying this effect.
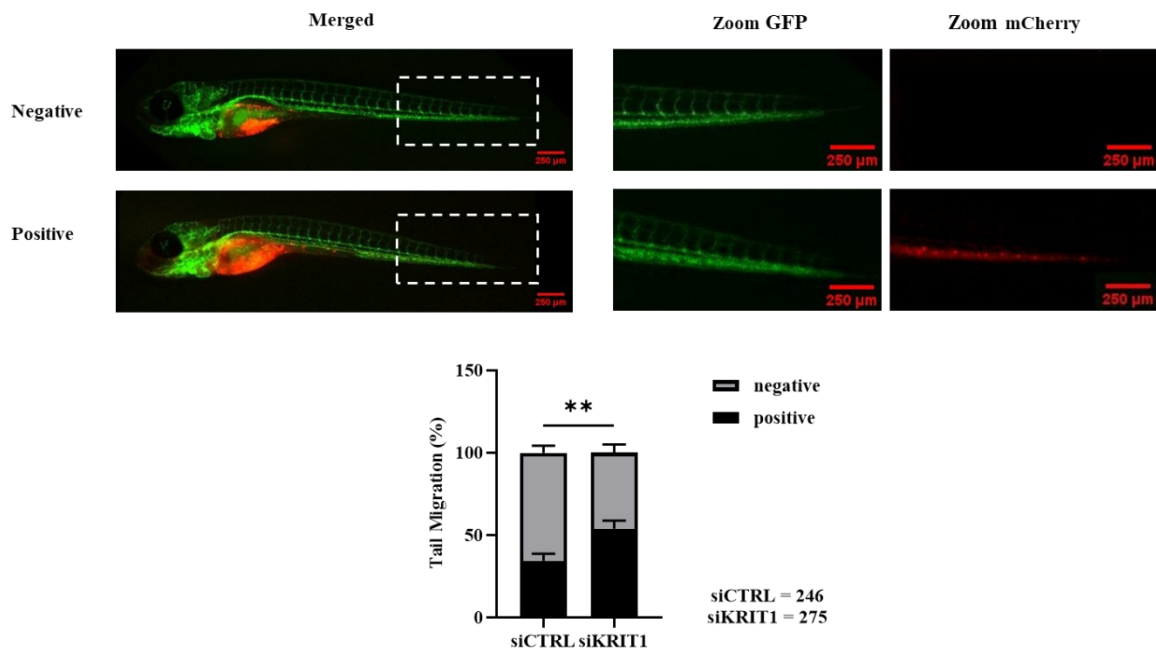

Figure 13. A375 depleted of KRIT1 has a greater ability to migrate in zebrafish
A375 transfected with siRNA against KRIT1, or negative control and stained red were injected into the yolk sac of zebrafish embryos. Fish with displaced cells in the tail were considered positive for migration, while those without were negative. The data shown in the figure are representative of three different experiments with a total of 246 fish for siCTRL and 275 for siKRIT1 (**$p<0,01$)

It is known that under pro-migratory conditions, KIF1C phosphorylation is observed in invadopodia and ensures their continuous elongation (Saji et al., 2022) and NS1A a known stabilizer of the cytoskeleton and actin filaments through direct binding to F-actin (Guazzi et al., 2012). To evaluate the interplay between KRIT1, KIF1C and NS1A we analyzed the levels of KIF1C phosphorylation, and KIF1C and NS1A expression in cancer cells silenced for KRIT1. Figure 14 shows that KRIT1 downregulation by siRNA corresponds to an increase in KIF1C phosphorylation, while we observed an inhibition of NS1A expression,

indicating a possible link between all these proteins. These data indicate that KRIT1, KIF1C and NS1A cooperate to promote cancer cell migration.
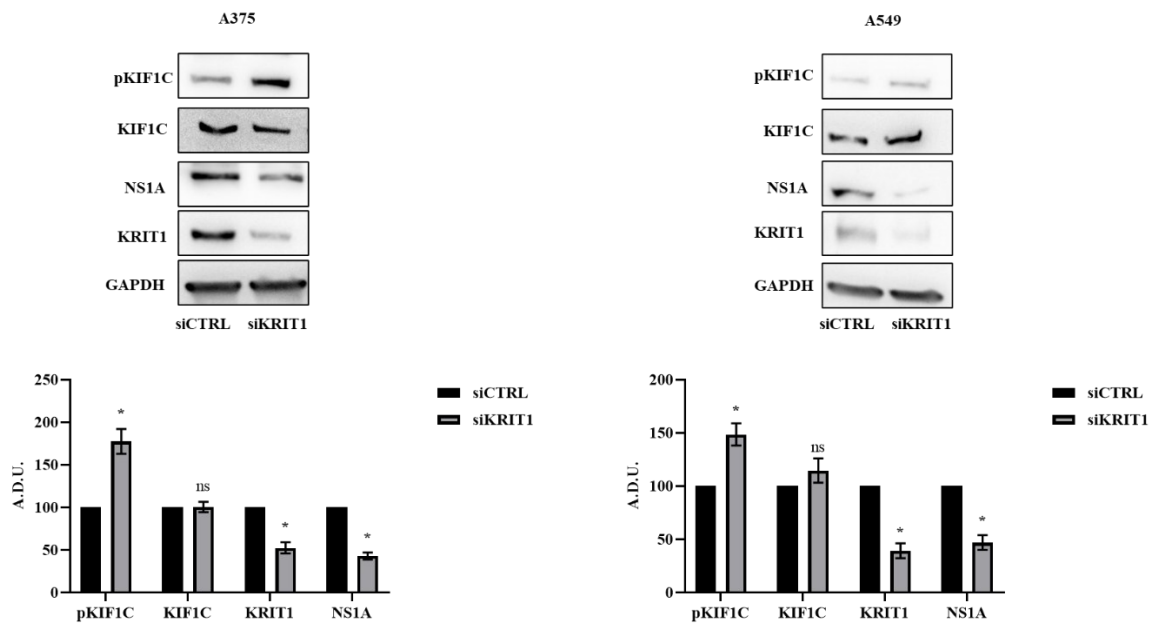

Figure 14. Correlation between KRIT1, KIF1C and NS1A
A375 and A549 cells were transfected with siRNA against KRIT1 for 72 h.
Images are representative of three independent experiments
*p<0,05

Given that the loss of KRIT1 promotes migration and is related to downregulation of the expression of NS1A we evaluated F-actin levels using immunofluorescence following KRIT1 silencing.

As shown in Figure 15, the loss of KRIT1 and NS1A is associated with an increase in the number of stress fibres and a subsequent alteration in cytoskeleton organization. These changes are critical for the acquisition of a migratory phenotype.
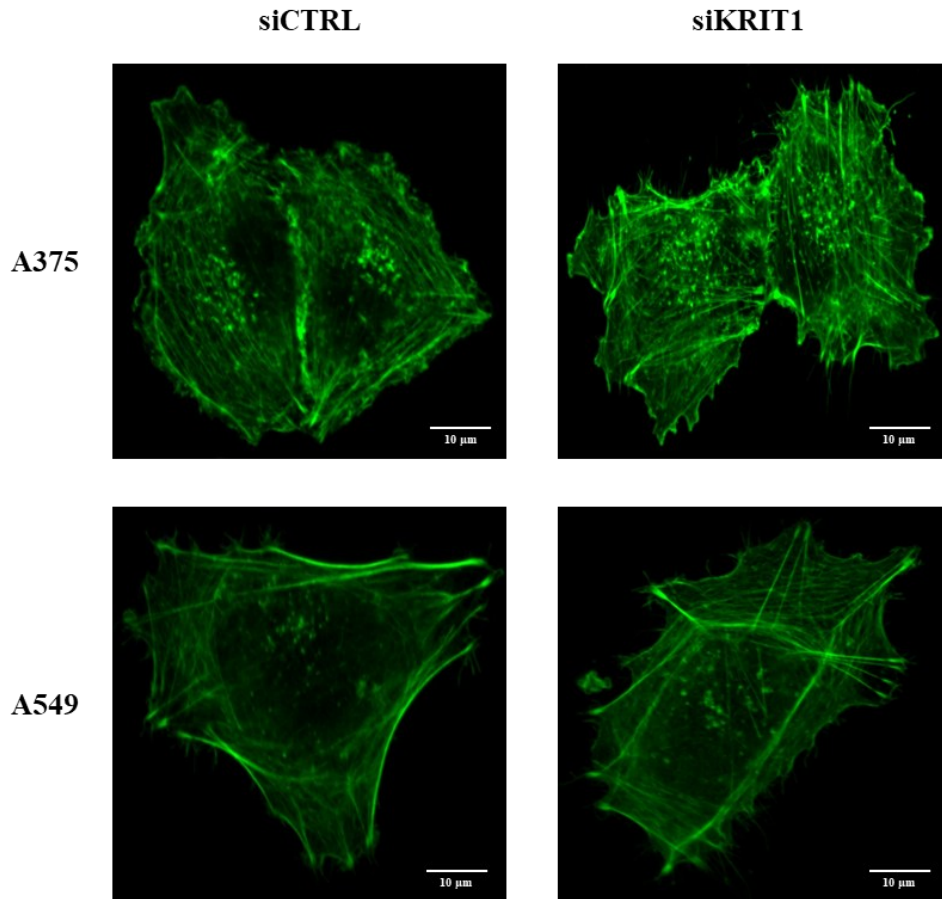
Figure 15. KRIT1 loss increases stress fibres formation
A375 and A549 were grown on coverslips, transfected with siRNA
against KRIT1 and then stained for Phalloidin

SRC family kinases have been shown to interconnect various cellular pathways that promote invasion and metastasis. Unsurprisingly, these pathways are also critical for the initiation and propagation of the epithelial-to-mesenchymal transition. EMT is a cellular program that enables epithelial cells to acquire mesenchymal features and plays a crucial role in embryonic development, wound healing, and malignant progression (Ortiz et al., 2021). SRC family kinases are key regulators of cell morphology and epithelial integrity, primarily through their role in actin cytoskeletal dynamics and cellular adhesions. EMT is characterized by morphological changes resulting from the loss of cell–cell junctions and actin-cytoskeleton rearrangement. SRC promotes cellular junction disassembly by activating focal adhesion kinase (Ortiz et al., 2021). Additionally, c-SRC-mediated phosphorylation of KIF1C has been observed to increases KIF1C binding to microtubules promoting invadopodia elongation in cancer cells (Saji et al., 2022). Starting from these observations, we investigated whether KRIT1 downregulation induces SRC and FAK phosphorylation.
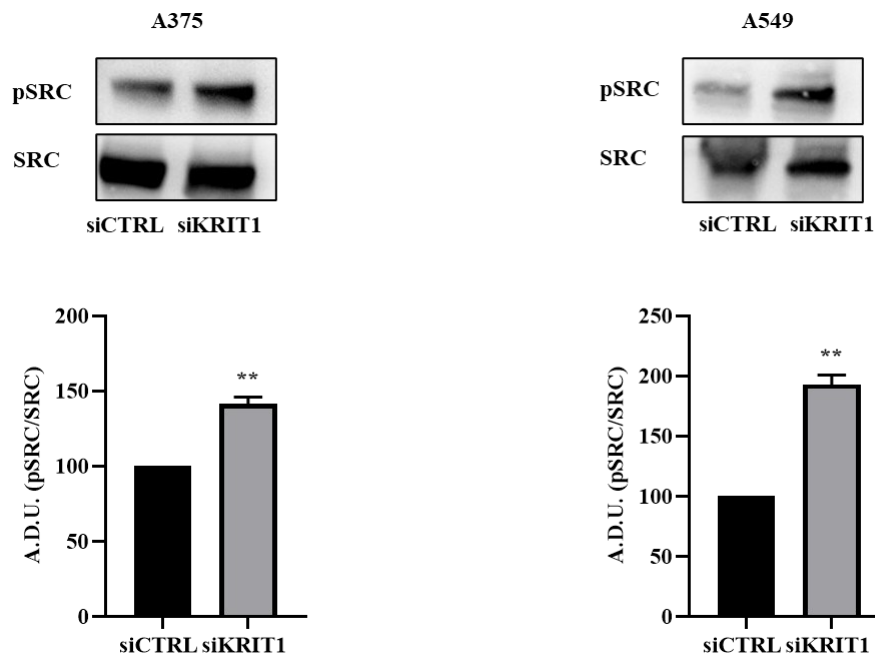
A375

pSRC

SRC

siCTRL siKRIT1

A549

pSRC

SRC

siCTRL siKRIT1

Figure 126. KRIT1 loss activates the SRC pathway
A375 and A549 cells were transfected with siRNA against KRIT1 for 72 h.
Cell lysates were then analyzed by Western blotting against SRC and pSRC.
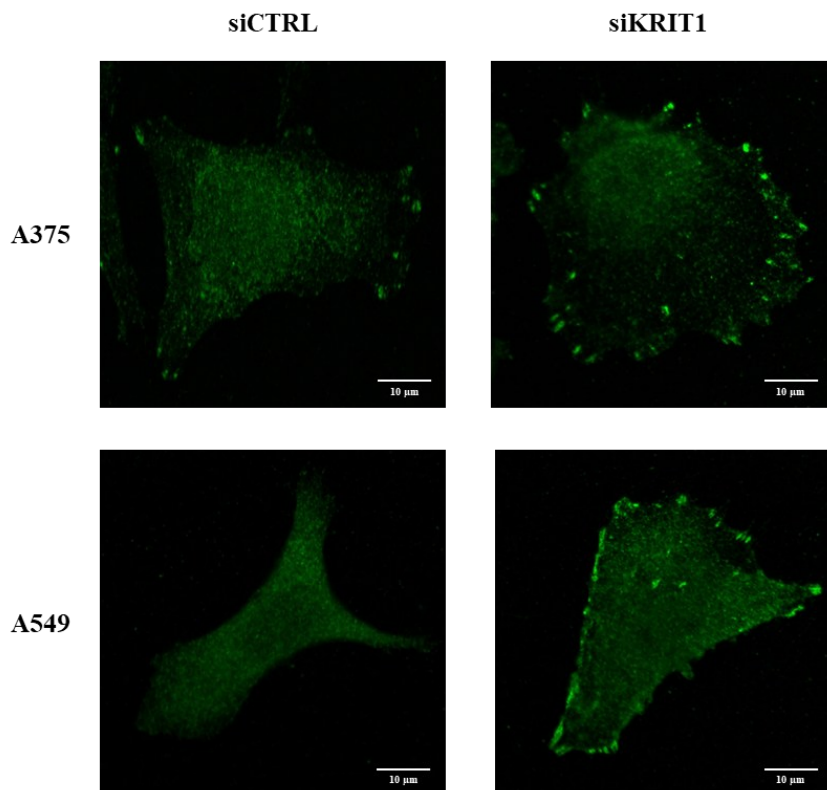Images are representative of three independent experiments
**p<0,01

siCTRL siKRIT1

A375

A549

Figure 17. KRIT1 loss induces FAK phosphorylation
A375 and A549 were grown on coverslips, transfected with siRNA
against KRIT1, and finally stained for pFAK

As shown in Figures 16 and 17, SRC and FAK become phosphorylated in cancer cells with low KRIT1 expression, suggesting a role of these kinases in cell migration driven by KRIT1 loss.

The Rho family of small GTPases and ROCK are well-established regulators of actin cytoskeleton organization and dynamics, playing key roles in cell motility and contributing to metastasis (Matsuoka, 2014). In particular, RhoA is crucial for regulating actin polymerization, membrane bleb formations, turnover of cell-extracellular matrix adhesions at the cell rear, basement membrane disassembly, and cortical contractility. RhoC promotes metastasis by regulating actin polymerization within invadopodia protrusions, whereas RhoB acts as a metastasis inhibitor (Wheeler and Ridley, 2004). In epithelial cells, KRIT1 has been identified as a negative regulator of RhoA and ROCK. Loss of KRIT1 can lead to MLC phosphorylation and subsequent stress fiber formation (Stockton et al., 2010). To investigate the effect of KRIT1 on Rho signaling in our cellular models, we assessed the expression levels of RhoA, RhoC and ROCK after KRIT1 silencing by Western blot analysis. Figure 18 shows that RhoA and ROCK expression increased in the absence of KRIT1, while the expression of RhoC did not change significantly. These results confirm that KRIT1 acts as a negative regulator of RhoA and ROCK in cancer cells, suggesting its involvement in cytoskeleton dynamics and cell motility. As Nd1-L also appears to suppress the activation of RhoA, Rac and CdC41 (Hatano, 2009), the KRIT1/NS1A interaction could be relevant for the mechanism proposed.
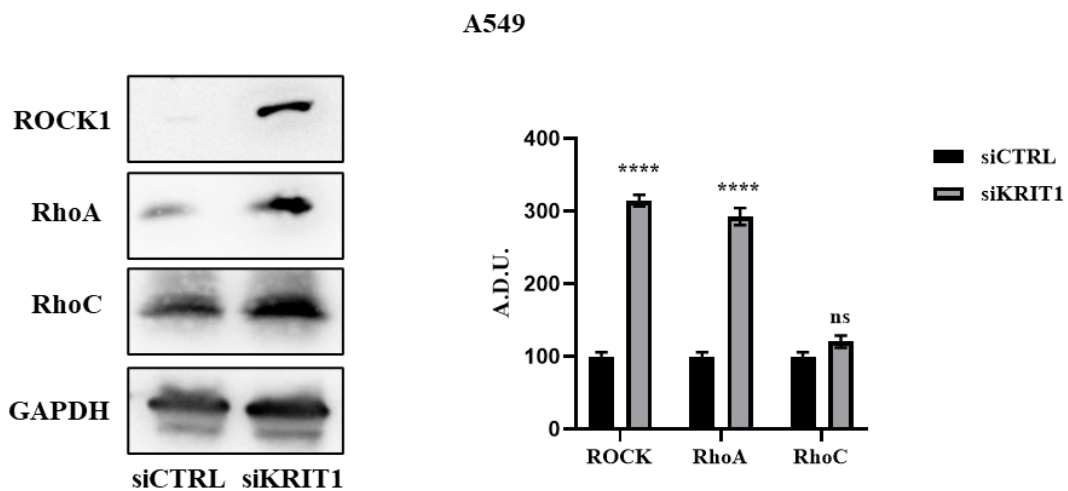

Figure 138. In cancer cells, KRIT1 functions as a negative regulator of RhoA and ROCK
A375 and A549 cells were transfected with siRNA against KRIT1 for 72 h.
Images are representative of three independent experiments
****p<0,0001

To further explore the role of KRIT1 in invasive phenotype of cancer cells, the invasion of spheroids formed by tumor cells and fibroblasts into a matrix composed of collagen and matrigel was assessed. The previously used cell lines were replaced by others with highly invasive capabilities, as they were positive for integrin αvβ6 (also called integrin β6) expression (Capan1, H358, H441 and H2009), with the exception of AsPC1, which was negative. The expression of the integrin β6 heterodimer is restricted to epithelial cells, where it acts as a receptor for fibronectin, tenascin, and latency-associated peptide, a protein that helps maintain tumor growth factor-β in its inactive form. Integrin β6 levels are increased during wound healing and in various epithelial tumors. In oral squamous cell carcinoma (SCC), β6 expression has been associated with tumor cell invasion both *in vitro* and *in vivo*. Additionally, β6 has been shown to regulate the production of various matrix metalloproteinases, particularly MMP-9 and MMP-3, in different tumor types and in normal keratinocytes. While there is significant homology between integrin β-subunits, the β6 subunit is distinguished by a unique 11-amino acid sequence at its C-terminus (EKQKVDLSTDC). This sequence is not only critical for β6-mediated invasion, but it is also sufficient to enhance invasive behavior through the upregulation of gelatinases. Notably, the specific gelatinase that is upregulated depends on the integrin's cytoplasmic tail to which this 11-amino acid sequence is attached, rather than the sequence itself (Morgan et al., 2004). Spheroid co-cultures were generated by resuspension of fibroblasts (MRC5 and PS1) and cancer cells (AsPC1, Capan1, H358, H441 and H2009) in hanging droplets containing methylcellulose. Cancer cells were previously transfected with siRNA against KRIT1, KIF1C, or NS1A. The following day, spheroids were collected and embedded in a 3D matrix in glass-bottomed 96-well plates. Invasion of cells from the center of the spheroid into the surrounding matrix was monitored by light microscopy. Deletion of KRIT1 increased the ability of cancer cells to invade into the matrix in co-culture with fibroblast (Figure 19). Interestingly, the increased invasion was only observed in integrin β6-positive tumor cells. Loss of KRIT1 may therefore enhance the effect of this integrin on invasion. Further studies are needed to confirm this hypothesis. Loss of KIF1C does not increase invasion, in line with the fact that phosphorylation and not depletion of this protein is observed in tumor cells with a more aggressive phenotype (Figure 20). And finally, reducing NS1A expression alone does not increase invasiveness. NS1A could only be involved in this phenomenon if KRIT1 was also depleted (Figure 21).
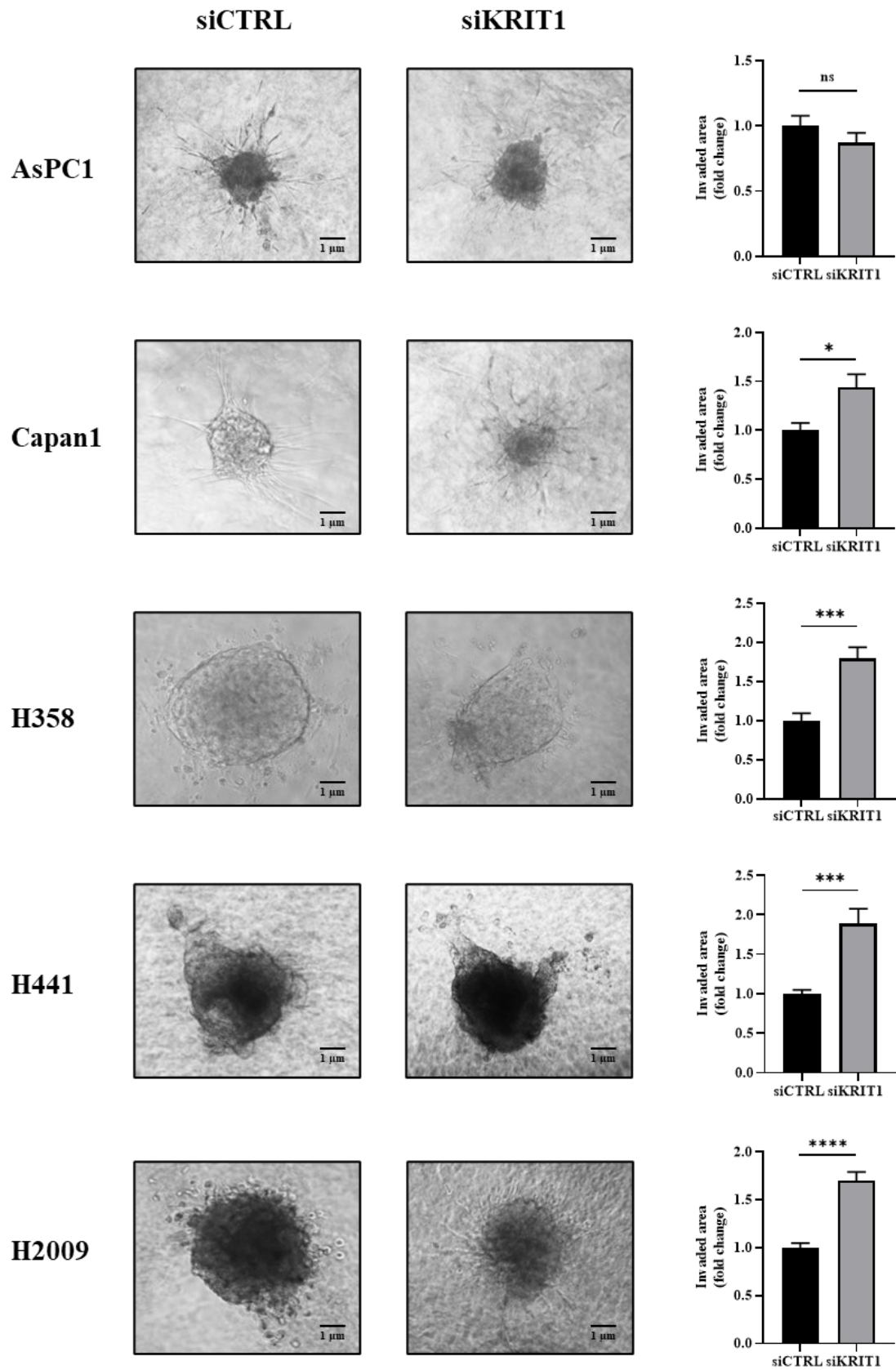
Figure 19. KRIT1 depletion induce an increase in invasion
Bright field of spheroids embedded in matrigel and collagen matrix after siRNA anti-KRIT1
treatment. Images are representative of three independent experiments
(*p<0,05; ***< 0,001; ****p<0,0001)

Figure 20. KIF1C loss does not affect tumor cell invasion
Bright field of spheroids embedded in matrigel and collagen matrix after siRNA anti-KIF1C treatment.
Images are representative of three independent experiments
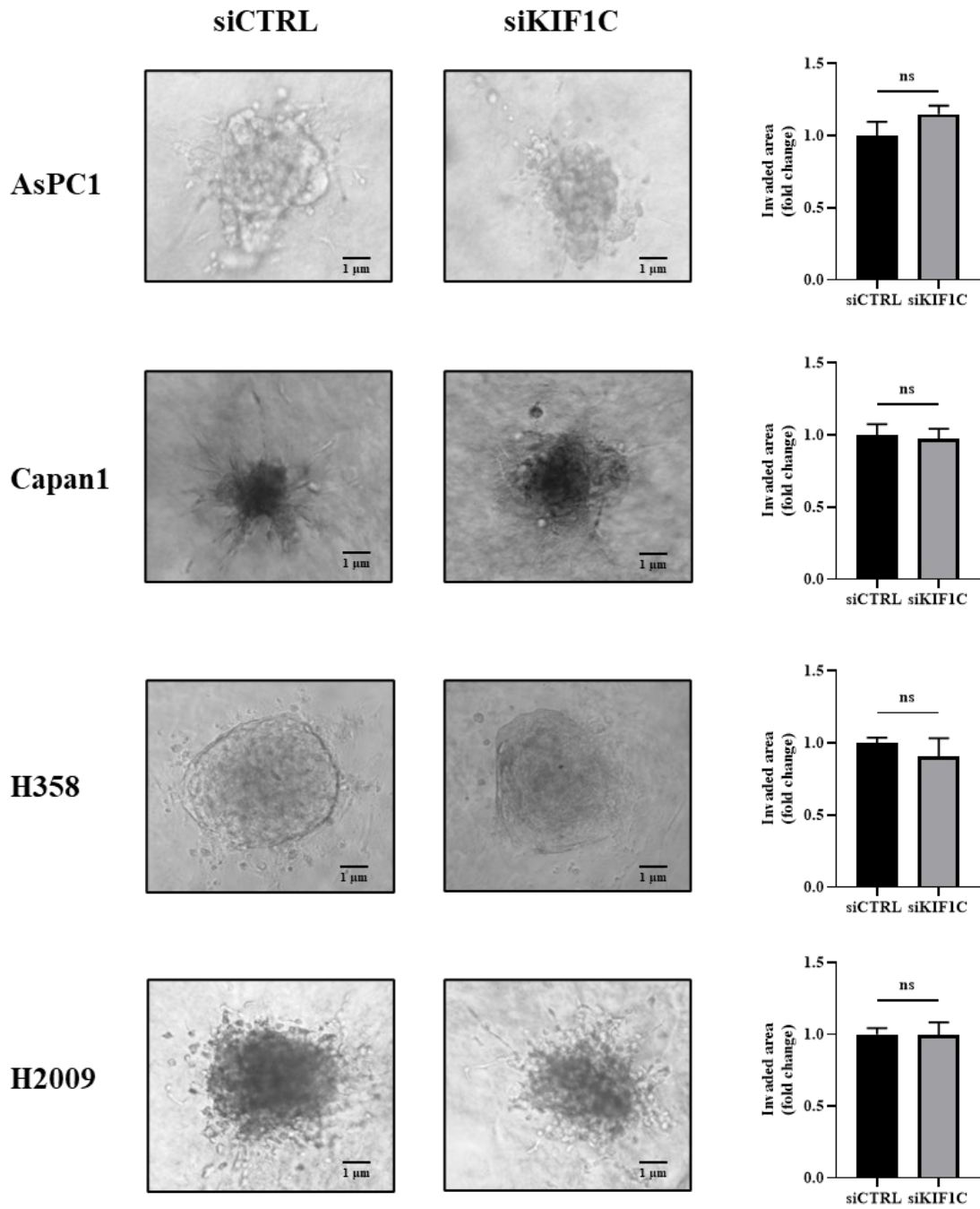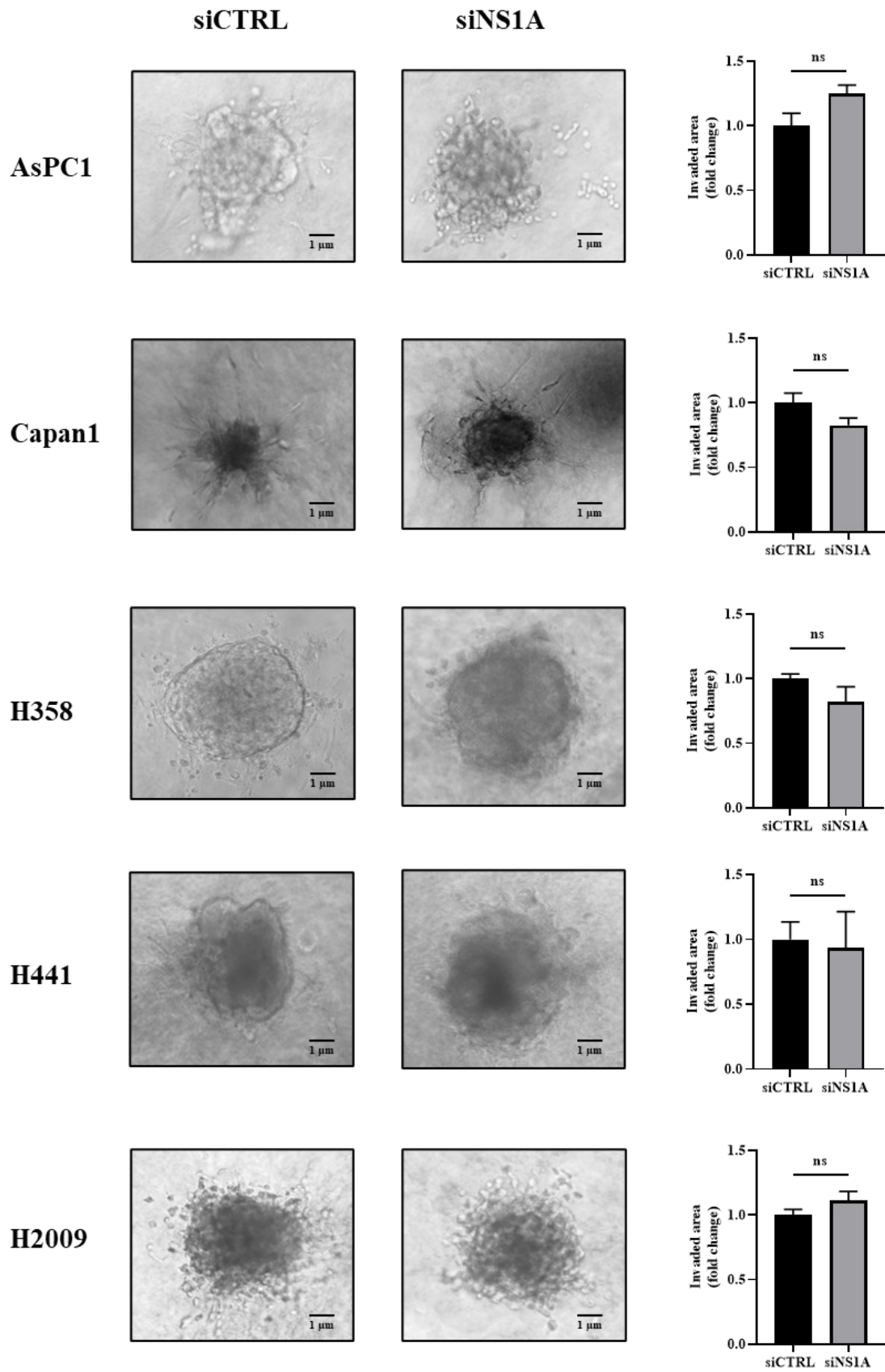
Figure 21. NS1A loss does not affect tumor cell invasion
Bright field of spheroids embedded in matrigel and collagen matrix after siRNA anti-NS1A treatment.
Images are representative of three independent experiments

5. CONCLUSIONS

KRIT1 is a scaffold protein lacking catalytic domains but containing several protein-protein interaction motifs that mediate the formation of functional complexes involved in physiologically important signaling networks (Su and Calderwood, 2020). KRIT1 has been extensively studied, as mutations in its gene are associated with Cerebral Cavernous Malformations, a rare vascular disorder that primarily affects the central nervous system. CCMs are characterized by abnormally dilated, leaky capillaries with a thin endothelial lining and a lack of normal structural integrity. KRIT1 regulates multiple signaling pathways involved in cell-cell interactions, cytoskeleton dynamics, angiogenesis, oxidative stress, and inflammation (Retta et al., 2020). Moreover, KRIT1 plays a crucial role in cell motility and migration, influencing not only endothelial cells but also non-endothelial cells, such as cancer cells (Ercoli et al., 2020) and neutrophils (Nobiletti et al., 2023).

KRIT1 is increasingly recognized as a tumor suppressor gene, with several studies supporting its role in inhibiting cancer progression. In mice with hemizygous KRIT1 deficiency, the loss of a single KRIT1 allele resulted in an increased incidence of small intestinal adenomas and reduced survival compared to controls. This deficiency led to the dissociation of β-catenin from vascular endothelial (VE)-cadherin, its accumulation in the nucleus, and the activation of β-catenin-dependent transcription (Glading and Ginsberg, 2010). In primary tumors, an inverse correlation between KRIT1 and miR-21 expression was observed. miR-21, an oncogenic microRNA overexpressed in tumors, is thought to target KRIT1, which may counteract miR-21's pro-tumor effects (Orso et al., 2013). In melanoma, reduced KRIT1 expression is associated with increased tumor aggressiveness. KRIT1 knockdown led to upregulation of N-cadherin and vimentin, proteins involved in the EMT, thereby contributing to melanoma plasticity. KRIT1 loss also enhances melanoma cell growth, migration, and invasion (Ercoli et al., 2020). Furthermore, colon cancer cells regulate KRIT1 expression in endothelial cells via exosomes. Specifically, exosomal miR-21-5p directly suppresses KRIT1 in the endothelium, promoting tumor angiogenesis and vascular permeability, which fuels tumor progression (He et al., 2021).

In this work we evaluated the role of KRIT1 in two fundamental aspects of cancer research: cellular invasion and migration. Specifically, we focused on the physiopathological significance of two recently identified KRIT1 molecular interactions: KRIT1/Nd1-L and KRIT1/KIF1C.

Nd1-L was previously identified as a novel KRIT1 binding partner by Guazzi et al. through yeast two-hybrid screening of a mouse embryo cDNA library (Guazzi et al., 2012). Similarly, another yeast two-hybrid screening identified KIF1C, a member of the kinesin superfamily, as a potential binding partner of KRIT1. The KRIT1/KIF1C interaction, initially isolated in the screening, was validated through pull-down and co-immunoprecipitation assays using recombinant proteins, and by co-immunoprecipitation of endogenous proteins in human endothelial cells (Trabalzini et al. manuscript in preparation).

In this study, to further characterize the newly discovered interaction and map the regions of KRIT1 involved in binding to KIF1C, both a GST pull-down assay and an in vitro ELISA format binding assay were performed using different KRIT1 fragments: the C-terminal region containing the FERM domain, the N-terminal fragment with three NPXY/F motifs, and full-length KRIT1. We demonstrated that full-length KRIT1, as well as its N- and C-terminal fragments bind to KIF1C, albeit with varying affinities. Specifically, full-length KRIT1 exhibited the highest binding affinity, followed by the KRIT1A FERM domain, which showed a stronger interaction with KIF1C than the N-terminal fragment.

Bimodal interaction was further supported by in silico analysis, which emphasized the critical role of the FERM domain in mediating the interaction between KRIT1 and KIF1C.

The two recently identified KRIT1 binding partners, Nd1-L and KIF1C are both involved in the regulation of cytoskeleton dynamics and rearrangements associated with cell movement and cancer progression potentially mediating KRIT1 functions in these processes. Nd1-L, an F-actin stabilizing protein, acts as a suppressor of RhoA, Rac, and Cdc42 (Hatano, 2009; Guazzi et al., 2012). KIF1C, through its phosphorylated form mediated by c-SRC, enhances its binding to microtubules and promotes invadopodia elongation in cancer cells (Saji et al., 2022). KRIT1 regulates cytoskeletal dynamics and serves as a negative regulator of RhoA and ROCK in endothelial cells (Stockton et al., 2010).

The interactions between KRIT1/KIF1C and KRIT1/NS1A (the human homolog of Nd1-L) have been observed in human cancer cell lines (A375 and A549) through co-immunoprecipitation assays. KRIT1, KIF1C, and NS1A were found to colocalize with β-tubulin, underscoring their association with the cytoskeleton. Furthermore, the loss of KRIT1 was shown to increase the metastatic potential of cancer cells, both *in vitro* and *in vivo*, a process accompanied by the phosphorylation of KIF1C and a decrease in NS1A expression. These findings suggest that KRIT1, KIF1C, and NS1A collaborate to regulate cancer cell migration.

In cancer cells, KRIT1 loss was associated with an increase in stress fibres, phosphorylation of SRC and FAK, and activation of the RhoA/ROCK pathway. These results underscore the pivotal role of KRIT1, in cooperation with binding partners, in regulating cytoskeletal dynamics and cell motility.

Taken together the data presented in this study expand our understanding of the molecular mechanisms underlying the anticancer activities of KRIT1. They also propose a potential molecular pathway involved in the acquisition of an aggressive phenotype, providing a scientific foundation for further therapeutic strategies and new potential targets for cancer treatment.

6. LIST OF ABBREVIATIONS

AF-6	Afadin
ARD	Ankyrin repeat domain
BCA	Bicinchoninic acid assay
BSA	Bovine serum albumin
CAF	Cancer-associated fibroblast
CCM	Cerebral Cavernous Malformations
CNS	Central nervous system
COX2	Cyclooxygenase 2
CRMP2	Collapsing response mediator protein 2
CSC	Cancer steam cell
CTL	Cytotoxic T lymphocytes
DMEM	Dulbecco's Modified Eagle Medium
EC	Endothelial cell
ECM	Extracellular matrix
EMEM	Eagle's minimum essential medium
EMT	Epithelial-mesenchymal transition
ERK	Extracellular signal-regulated kinase
ERM	Ezrin/radixin/moesin proteins
FAK	Focal adhesion kinase
FBS	Fetal bovine serum
FoxO1	Forkhead box protein O1
GAP	GTPase-activating proteins
GDI	Guanine nucleotide dissociation inhibitors
GEF	Guanine nucleotide exchange factors
HEG1	Heart-of-Glass receptor
HPF	Hours post fertilization
ICAP1α	Integrin cytoplasmic domain associated protein-1
JNK	Jun N-terminal kinase
K1Afull	KRIT1A full length
KF1A	Residues 418-736 of KRIT1A FERM domain
KIF	Kinesin superfamily
KNT272	Residues 1-272 of KRIT1

LIMK	LIM kinase
MAPK	Mitogen-activated protein kinases
mCRPC	Metastatic castration-resistant prostate cancer
MLC	Myosin light chain
MLCK	Myosin light chain kinase
MMP	Matrix Metalloproteinases
m-PGES1	Microsomal prostaglandin E synthase 1
MYPT1	Myosin phosphatase 1
Nd1-L	Influenza virus NS1A-binding protein
NK	Natural killer
OV	Overall survival
PBS	Phosphate buffered saline
PFA	Paraformaldehyde
PGE2	Prostaglandin E2
PM	Plasma membrane
PMA	Phorbol 12-myristate 13-acetate
pMLC	Phosphorylated myosin light chain
PTP	Protein tyrosine phosphatases
ROCK	Rho-associated serine/threonine kinase
ROS	Reactive oxygen species
RTK	Receptor tyrosine kinases
SCC	Squamous cell carcinoma
SOD	Superoxide dismutase
TME	Tumor microenvironment
UT	Untransfected cells

7. BIBLIOGRAPHY

Abraham, M.J., Murtola, T., Schulz, R., Páll, S., Smith, J.C., Hess, B., Lindahl, E., 2015. GROMACS: High performance molecular simulations through multi-level parallelism from laptops to supercomputers. SoftwareX 1–2, 19–25. https://doi.org/10.1016/j.softx.2015.06.001

Adams, J., Kelso, R., Cooley, L., 2000. The kelch repeat superfamily of proteins: propellers of cell function. Trends Cell Biol. 10, 17–24. https://doi.org/10.1016/S0962-8924(99)01673-6

Aiello, N.M., Maddipati, R., Norgard, R.J., Balli, D., Li, J., Yuan, S., Yamazoe, T., Black, T., Sahmoud, A., Furth, E.E., Bar-Sagi, D., Stanger, B.Z., 2018. EMT Subtype Influences Epithelial Plasticity and Mode of Cell Migration. Dev. Cell 45, 681-695.e4. https://doi.org/10.1016/j.devcel.2018.05.027

Amano, M., Nakayama, M., Kaibuchi, K., 2010. Rho-kinase/ROCK: A key regulator of the cytoskeleton and cell polarity. Cytoskelet. Hoboken NJ 67, 545–554. https://doi.org/10.1002/cm.20472

Antognelli, C., Trapani, E., Delle Monache, S., Perrelli, A., Fornelli, C., Retta, F., Cassoni, P., Talesa, V.N., Retta, S.F., 2018. Data in support of sustained upregulation of adaptive redox homeostasis mechanisms caused by KRIT1 loss-of-function. Data Brief 16, 929–938. https://doi.org/10.1016/j.dib.2017.12.026

Bardwell, V.J., Treisman, R., 1994. The POZ domain: a conserved protein-protein interaction motif. Genes Dev. 8, 1664–1677. https://doi.org/10.1101/gad.8.14.1664

Berrier, A.L., Yamada, K.M., 2007. Cell-matrix adhesion. J. Cell. Physiol. 213, 565–573. https://doi.org/10.1002/jcp.21237

Bjorge, J.D., Jakymiw, A., Fujita, D.J., 2000. Selected glimpses into the activation and function of Src kinase. Oncogene 19, 5620–5635. https://doi.org/10.1038/sj.onc.1203923

Boulter, E., Garcia-Mata, R., Guilluy, C., Dubash, A., Rossi, G., Brennwald, P.J., Burridge, K., 2010. Regulation of Rho GTPase crosstalk, degradation and activity by RhoGDI1. Nat. Cell Biol. 12, 477–483. https://doi.org/10.1038/ncb2049

Brown, J.S., Amend, S.R., Austin, R.H., Gatenby, R.A., Hammarlund, E.U., Pienta, K.J., 2023. Updating the Definition of Cancer. Mol. Cancer Res. 21, 1142–1147. https://doi.org/10.1158/1541-7786.MCR-23-0411

Calderwood, D.A., 2004. Talin controls integrin activation. Biochem. Soc. Trans. 32, 434–437. https://doi.org/10.1042/BST0320434

Calderwood, D.A., Tai, V., Di Paolo, G., De Camilli, P., Ginsberg, M.H., 2004. Competition for talin results in trans-dominant inhibition of integrin activation. J. Biol. Chem. 279, 28889–28895. https://doi.org/10.1074/jbc.M402161200

Choi, P.-W., Yang, J., Ng, S.-K., Feltmate, C., Muto, M.G., Hasselblatt, K., Lafferty-Whyte, K., JeBailey, L., MacConaill, L., Welch, W.R., Fong, W.-P., Berkowitz, R.S., Ng, S.-W., 2016. Loss of E-cadherin disrupts ovarian epithelial inclusion cyst formation and collective cell movement in ovarian cancer cells. Oncotarget 7, 4110–4121. https://doi.org/10.18632/oncotarget.6588

Chuai, M., Hughes, D., J. Weijer, C., 2012. Collective Epithelial and Mesenchymal Cell Migration During Gastrulation. Curr. Genomics 13, 267–277. https://doi.org/10.2174/138920212800793357

Clark, E.A., Golub, T.R., Lander, E.S., Hynes, R.O., 2000. Genomic analysis of metastasis reveals an essential role for RhoC. Nature 406, 532–535. https://doi.org/10.1038/35020106

Coffelt, S.B., Lewis, C.E., Naldini, L., Brown, J.M., Ferrara, N., De Palma, M., 2010. Elusive Identities and Overlapping Phenotypes of Proangiogenic Myeloid Cells in Tumors. Am. J. Pathol. 176, 1564–1576. https://doi.org/10.2353/ajpath.2010.090786

Cramer, L.P., 1999. Organization and polarity of actin filament networks in cells: implications for the mechanism of myosin-based cell motility. Biochem. Soc. Symp. 65, 173–205

Critchley, D.R., Gingras, A.R., 2008. Talin at a glance. J. Cell Sci. 121, 1345–1347. https://doi.org/10.1242/jcs.018085

De Visser, K.E., Joyce, J.A., 2023. The evolving tumor microenvironment: From cancer initiation to metastatic outgrowth. Cancer Cell 41, 374–403. https://doi.org/10.1016/j.ccell.2023.02.016

Denier, C., Gasc, J.-M., Chapon, F., Domenga, V., Lescoat, C., Joutel, A., Tournier-Lasserve, E., 2002. Krit1/cerebral cavernous malformation 1 mRNA is preferentially expressed in neurons and epithelial cells in embryo and adult. Mech. Dev. 117, 363–367. https://doi.org/10.1016/S0925-4773(02)00209-5

DiStefano, P.V., Kuebel, J.M., Sarelius, I.H., Glading, A.J., 2014. KRIT1 Protein Depletion Modifies Endothelial Cell Behavior via Increased Vascular Endothelial Growth Factor (VEGF) Signaling. J. Biol. Chem. 289, 33054–33065. https://doi.org/10.1074/jbc.M114.582304

Doye, A., Mettouchi, A., Lemichez, E., 2012. Assessing ubiquitylation of Rho GTPases in mammalian cells. Methods Mol. Biol. Clifton NJ 827, 77–86. https://doi.org/10.1007/978-1-61779-442-1_5

Draheim, K.M., Fisher, O.S., Boggon, T.J., Calderwood, D.A., 2014. Cerebral cavernous malformation proteins at a glance. J. Cell Sci. jcs.138388. https://doi.org/10.1242/jcs.138388

Efimova, N., Grimaldi, A., Bachmann, A., Frye, K., Zhu, X., Feoktistov, A., Straube, A., Kaverina, I., 2014. Podosome-regulating kinesin KIF1C translocates to the cell periphery in a CLASP-dependent manner. J. Cell Sci. jcs.149633. https://doi.org/10.1242/jcs.149633

Ercoli, J., Finetti, F., Woodby, B., Belmonte, G., Miracco, C., Valacchi, G., Trabalzini, L., 2020. KRIT1 as a possible new player in melanoma aggressiveness. Arch. Biochem. Biophys. 691, 108483. https://doi.org/10.1016/j.abb.2020.108483

Finetti, F., Schiavo, I., Ercoli, J., Zotta, A., Boda, E., Retta, S.F., Trabalzini, L., 2020. KRIT1 loss-mediated upregulation of NOX1 in stromal cells promotes paracrine pro-angiogenic responses. Cell. Signal. 68, 109527. https://doi.org/10.1016/j.cellsig.2020.109527

Finetti, F., Trabalzini, L., 2021. Non-autonomous effects of CCM genes loss. Vessel Plus. https://doi.org/10.20517/2574-1209.2021.49

Fisher, O.S., Boggon, T.J., 2014. Signaling pathways and the cerebral cavernous malformations proteins: lessons from structural biology. Cell. Mol. Life Sci. 71, 1881–1892. https://doi.org/10.1007/s00018-013-1532-9

Frame, M.C., Fincham, V.J., Carragher, N.O., Wyke, J.A., 2002. v-Src's hold over actin and cell adhesions. Nat. Rev. Mol. Cell Biol. 3, 233–245. https://doi.org/10.1038/nrm779

Francalanci, F., Avolio, M., De Luca, E., Longo, D., Menchise, V., Guazzi, P., Sgrò, F., Marino, M., Goitre, L., Balzac, F., Trabalzini, L., Retta, S.F., 2009. Structural and functional differences between KRIT1A and KRIT1B isoforms: A framework for understanding CCM pathogenesis. Exp. Cell Res. 315, 285–303. https://doi.org/10.1016/j.yexcr.2008.10.006

Friedl, P., Wolf, K., 2003. Tumour-cell invasion and migration: diversity and escape mechanisms. Nat. Rev. Cancer 3, 362–374. https://doi.org/10.1038/nrc1075

Gaengel, K., Genové, G., Armulik, A., Betsholtz, C., 2009. Endothelial-Mural Cell Signaling in Vascular Development and Angiogenesis. Arterioscler. Thromb. Vasc. Biol. 29, 630–638. https://doi.org/10.1161/ATVBAHA.107.161521

Gilbertson, R.J., Rich, J.N., 2007. Making a tumour's bed: glioblastoma stem cells and the vascular niche. Nat. Rev. Cancer 7, 733–736. https://doi.org/10.1038/nrc2246

Gingras, A.R., Ziegler, W.H., Bobkov, A.A., Joyce, M.G., Fasci, D., Himmel, M., Rothemund, S., Ritter, A., Grossmann, J.G., Patel, B., Bate, N., Goult, B.T., Emsley, J., Barsukov, I.L., Roberts, G.C.K., Liddington, R.C., Ginsberg, M.H., Critchley, D.R., 2009. Structural determinants of integrin binding to the talin rod. J. Biol. Chem. 284, 8866–8876. https://doi.org/10.1074/jbc.M805937200

Glading, A., Han, J., Stockton, R.A., Ginsberg, M.H., 2007. KRIT-1/CCM1 is a Rap1 effector that regulates endothelial cell–cell junctions. J. Cell Biol. 179, 247–254. https://doi.org/10.1083/jcb.200705175

Glading, A.J., Ginsberg, M.H., 2010. Rap1 and its effector KRIT1/CCM1 regulate β-catenin signaling. Dis. Model. Mech. 3, 73–83. https://doi.org/10.1242/dmm.003293

Goitre, L., De Luca, E., Braggion, S., Trapani, E., Guglielmotto, M., Biasi, F., Forni, M., Moglia, A., Trabalzini, L., Retta, S.F., 2014. KRIT1 loss of function causes a ROS-dependent upregulation of c-Jun. Free Radic. Biol. Med. 68, 134–147. https://doi.org/10.1016/j.freeradbiomed.2013.11.020

Goitre, L., DiStefano, P.V., Moglia, A., Nobiletti, N., Baldini, E., Trabalzini, L., Keubel, J., Trapani, E., Shuvaev, V.V., Muzykantov, V.R., Sarelius, I.H., Retta, S.F., Glading, A.J., 2017. Up-regulation of NADPH oxidase-mediated redox signaling contributes to the loss of barrier function in KRIT1 deficient endothelium. Sci. Rep. 7, 8296. https://doi.org/10.1038/s41598-017-08373-4

Goitre, L., Pergolizzi, B., Ferro, E., Trabalzini, L., Retta, S.F., 2012. Molecular Crosstalk between Integrins and Cadherins: Do Reactive Oxygen Species Set the Talk? J. Signal Transduct. 2012, 1–12. https://doi.org/10.1155/2012/807682

Gong, X., Didan, Y., Lock, J.G., Strömblad, S., 2018. KIF 13A-regulated RhoB plasma membrane localization governs membrane blebbing and blebby amoeboid cell migration. EMBO J. 37, e98994. https://doi.org/10.15252/embj.201898994

Goult, B.T., Bate, N., Anthis, N.J., Wegener, K.L., Gingras, A.R., Patel, B., Barsukov, I.L., Campbell, I.D., Roberts, G.C.K., Critchley, D.R., 2009. The Structure of an Interdomain Complex That Regulates Talin Activity. J. Biol. Chem. 284, 15097–15106. https://doi.org/10.1074/jbc.M900078200

Grinberg-Rashi, H., Ofek, E., Perelman, M., Skarda, J., Yaron, P., Hajdúch, M., Jacob-Hirsch, J., Amariglio, N., Krupsky, M., Simansky, D.A., Ram, Z., Pfeffer, R., Galernter, I., Steinberg, D.M., Ben-Dov, I., Rechavi, G., Izraeli, S., 2009. The Expression of Three Genes in Primary Non–Small Cell Lung Cancer Is Associated

with Metastatic Spread to the Brain. Clin. Cancer Res. 15, 1755–1761. https://doi.org/10.1158/1078-0432.CCR-08-2124

Guarino, M., 2010. Src signaling in cancer invasion. J. Cell. Physiol. 223, 14–26. https://doi.org/10.1002/jcp.22011

Guazzi, P., Goitre, L., Ferro, E., Cutano, V., Martino, C., Trabalzini, L., Retta, S.F., 2012. Identification of the Kelch Family Protein Nd1-L as a Novel Molecular Interactor of KRIT1. PLoS ONE 7, e44705. https://doi.org/10.1371/journal.pone.0044705

Gunel, M., Laurans, M.S.H., Shin, D., DiLuna, M.L., Voorhees, J., Choate, K., Nelson-Williams, C., Lifton, R.P., 2002. *KRIT1* , a gene mutated in cerebral cavernous malformation, encodes a microtubule-associated protein. Proc. Natl. Acad. Sci. 99, 10677–10682. https://doi.org/10.1073/pnas.122354499

Haeger, A., Alexander, S., Vullings, M., Kaiser, F.M.P., Veelken, C., Flucke, U., Koehl, G.E., Hirschberg, M., Flentje, M., Hoffman, R.M., Geissler, E.K., Kissler, S., Friedl, P., 2020. Collective cancer invasion forms an integrin-dependent radioresistant niche. J. Exp. Med. 217, e20181184. https://doi.org/10.1084/jem.20181184

Hanahan, D., Weinberg, R.A., 2011. Hallmarks of Cancer: The Next Generation. Cell 144, 646–674. https://doi.org/10.1016/j.cell.2011.02.013

Hatano, 2009. A kelch family protein Nd1-L functions as a metastasis suppressor in cancer cells via Rho family proteins mediated mechanism. Int. J. Oncol. 36. https://doi.org/10.3892/ijo_00000516

Haura, E.B., 2006. SRC and STAT pathways. J. Thorac. Oncol. Off. Publ. Int. Assoc. Study Lung Cancer 1, 403–405.

He, M., Cheng, Y., Li, W., Liu, Q., Liu, J., Huang, J., Fu, X., 2010. Vascular endothelial growth factor C promotes cervical cancer metastasis via up-regulation and activation of RhoA/ROCK-2/moesin cascade. BMC Cancer 10, 170. https://doi.org/10.1186/1471-2407-10-170

He, Q., Ye, A., Ye, W., Liao, X., Qin, G., Xu, Y., Yin, Y., Luo, H., Yi, M., Xian, L., Zhang, S., Qin, X., Zhu, W., Li, Y., 2021. Cancer-secreted exosomal miR-21-5p induces angiogenesis and vascular permeability by targeting KRIT1. Cell Death Dis. 12, 576. https://doi.org/10.1038/s41419-021-03803-8

Holle, A.W., Govindan Kutty Devi, N., Clar, K., Fan, A., Saif, T., Kemkemer, R., Spatz, J.P., 2019. Cancer Cells Invade Confined Microchannels via a Self-Directed Mesenchymal-to-Amoeboid Transition. Nano Lett. 19, 2280–2290. https://doi.org/10.1021/acs.nanolett.8b04720

Hotter, G., Mastora, C., Jung, M., Brüne, B., Carbonell, T., Josa, C., Pérez-Calvo, J.I., Cruzado, J.M., Guiteras, R., Sola, A., 2020. The influenza virus NS1A binding protein gene modulates macrophages response to cytokines and phagocytic potential in inflammation. Sci. Rep. 10, 15302. https://doi.org/10.1038/s41598-020-72342-7

Hynes, R.O., 2002. Integrins. Cell 110, 673–687. https://doi.org/10.1016/S0092-8674(02)00971-6

Ingley, E., 2008. Src family kinases: regulation of their activities, levels and identification of new pathways. Biochim. Biophys. Acta 1784, 56–65. https://doi.org/10.1016/j.bbapap.2007.08.012

Janson, G., Paiardini, A., 2021. PyMod 3: a complete suite for structural bioinformatics in PyMOL. Bioinformatics 37, 1471–1472. https://doi.org/10.1093/bioinformatics/btaa849

Jo, S., Kim, T., Iyer, V.G., Im, W., 2008. CHARMM-GUI: A web-based graphical user interface for CHARMM. J. Comput. Chem. 29, 1859–1865. https://doi.org/10.1002/jcc.20945

Jumper, J., Evans, R., Pritzel, A., Green, T., Figurnov, M., Ronneberger, O., Tunyasuvunakool, K., Bates, R., Žídek, A., Potapenko, A., Bridgland, A., Meyer, C., Kohl, S.A.A., Ballard, A.J., Cowie, A., Romera-Paredes, B., Nikolov, S., Jain, R., Adler, J., Back, T., Petersen, S., Reiman, D., Clancy, E., Zielinski, M., Steinegger, M., Pacholska, M., Berghammer, T., Bodenstein, S., Silver, D., Vinyals, O., Senior, A.W., Kavukcuoglu, K., Kohli, P., Hassabis, D., 2021. Highly accurate protein structure prediction with AlphaFold. Nature 596, 583–589. https://doi.org/10.1038/s41586-021-03819-2

Kamai, T., Kawakami, S., Koga, F., Arai, G., Takagi, K., Arai, K., Tsujii, T., Yoshida, K.-I., 2003. RhoA is associated with invasion and lymph node metastasis in upper urinary tract cancer. BJU Int. 91, 234–238. https://doi.org/10.1046/j.1464-410x.2003.03063.x

Kang, M., Matsudo, Y., Sasagawa, K., Tokuhisa, T., Hatano, M., 2001. Nd1, a novel murine Kelch family protein, may play the role of a housekeeping gene. Biochim. Biophys. Acta BBA - Gene Struct. Expr. 1519, 167–174. https://doi.org/10.1016/S0167-4781(01)00231-7

Katoh, K., Kano, Y., Amano, M., Onishi, H., Kaibuchi, K., Fujiwara, K., 2001. Rho-Kinase–Mediated Contraction of Isolated Stress Fibers. J. Cell Biol. 153, 569–584.

Klemke, R.L., Leng, J., Molander, R., Brooks, P.C., Vuori, K., Cheresh, D.A., 1998. CAS/Crk coupling serves as a "molecular switch" for induction of cell migration. J. Cell Biol. 140, 961–972. https://doi.org/10.1083/jcb.140.4.961

Kopp, P., Lammers, R., Aepfelbacher, M., Woehlke, G., Rudel, T., Machuy, N., Steffen, W., Linder, S., 2006. The Kinesin KIF1C and Microtubule Plus Ends Regulate Podosome Dynamics in Macrophages. Mol. Biol. Cell 17, 2811–2823. https://doi.org/10.1091/mbc.e05-11-1010

Krissinel, E., 2010. Crystal contacts as nature's docking solutions. J. Comput. Chem. 31, 133–143. https://doi.org/10.1002/jcc.21303

Liu, N., Zhang, G., Bi, F., Pan, Y., Xue, Y., Shi, Y., Yao, L., Zhao, L., Zheng, Y., Fan, D., 2007. RhoC is essential for the metastasis of gastric cancer. J. Mol. Med. 85, 1149–1156. https://doi.org/10.1007/s00109-007-0217-y

Liu, X., Gong, H., Huang, K., 2013. Oncogenic role of kinesin proteins and targeting kinesin therapy. Cancer Sci. 104, 651–656. https://doi.org/10.1111/cas.12138

Lorentzen, A., Bamber, J., Sadok, A., Elson-Schwab, I., Marshall, C.J., 2011. An ezrin-rich, rigid uropod-like structure directs movement of amoeboid blebbing cells. J. Cell Sci. 124, 1256–1267. https://doi.org/10.1242/jcs.074849

Maaser, K., Wolf, K., Klein, C.E., Niggemann, B., Zänker, K.S., Bröcker, E.-B., Friedl, P., 1999. Functional Hierarchy of Simultaneously Expressed Adhesion Receptors: Integrin α2β1 but Not CD44 Mediates MV3 Melanoma Cell Migration and Matrix Reorganization within Three-dimensional Hyaluronan-containing Collagen Matrices. Mol. Biol. Cell 10, 3067–3079. https://doi.org/10.1091/mbc.10.10.3067

Madaule, P., Axel, R., 1985. A novel ras-related gene family. Cell 41, 31–40. https://doi.org/10.1016/0092-8674(85)90058-3

Matsui, T., Maeda, M., Doi, Y., Yonemura, S., Amano, M., Kaibuchi, K., Tsukita, S., Tsukita, S., 1998. Rho-kinase phosphorylates COOH-terminal threonines of ezrin/radixin/moesin (ERM) proteins and regulates their head-to-tail association. J. Cell Biol. 140, 647–657. https://doi.org/10.1083/jcb.140.3.647

Matsuoka, T., 2014. Rho/ROCK signaling in motility and metastasis of gastric cancer. World J. Gastroenterol. 20, 13756. https://doi.org/10.3748/wjg.v20.i38.13756

Mayor, R., Etienne-Manneville, S., 2016. The front and rear of collective cell migration. Nat. Rev. Mol. Cell Biol. 17, 97–109. https://doi.org/10.1038/nrm.2015.14

McLean, G.W., Carragher, N.O., Avizienyte, E., Evans, J., Brunton, V.G., Frame, M.C., 2005a. The role of focal-adhesion kinase in cancer - a new therapeutic opportunity. Nat. Rev. Cancer 5, 505–515. https://doi.org/10.1038/nrc1647

McLean, G.W., Carragher, N.O., Avizienyte, E., Evans, J., Brunton, V.G., Frame, M.C., 2005b. The role of focal-adhesion kinase in cancer - a new therapeutic opportunity. Nat. Rev. Cancer 5, 505–515. https://doi.org/10.1038/nrc1647

Morgan, M.R., Thomas, G.J., Russell, A., Hart, I.R., Marshall, J.F., 2004. The Integrin Cytoplasmic-tail Motif EKQKVDLSTDC Is Sufficient to Promote Tumor Cell Invasion Mediated by Matrix Metalloproteinase (MMP)-2 or MMP-9 *. J. Biol. Chem. 279, 26533–26539. https://doi.org/10.1074/jbc.M401736200

Nagai, T., Ishikawa, T., Minami, Y., Nishita, M., 2020. Tactics of cancer invasion: solitary and collective invasion. J. Biochem. (Tokyo) 167, 347–355. https://doi.org/10.1093/jb/mvaa003

Nobiletti, N., Liu, J., Glading, A.J., 2023. KRIT1 -mediated regulation of neutrophil adhesion and motility. FEBS J. 290, 1078–1095. https://doi.org/10.1111/febs.16627

Orso, F., Balzac, F., Marino, M., Lembo, A., Retta, S.F., Taverna, D., 2013. miR-21 coordinates tumor growth and modulates KRIT1 levels. Biochem. Biophys. Res. Commun. 438, 90–96. https://doi.org/10.1016/j.bbrc.2013.07.031

Ortiz, M.A., Mikhailova, T., Li, X., Porter, B.A., Bah, A., Kotula, L., 2021. Src family kinases, adaptor proteins and the actin cytoskeleton in epithelial-to-mesenchymal transition. Cell Commun. Signal. 19, 67. https://doi.org/10.1186/s12964-021-00750-x

Paluch, E., Piel, M., Prost, J., Bornens, M., Sykes, C., 2005. Cortical Actomyosin Breakage Triggers Shape Oscillations in Cells and Cell Fragments. Biophys. J. 89, 724–733. https://doi.org/10.1529/biophysj.105.060590

Paluch, E.K., Raz, E., 2013. The role and regulation of blebs in cell migration. Curr. Opin. Cell Biol. 25, 582–590. https://doi.org/10.1016/j.ceb.2013.05.005

Park, S., Lee, H.-Y., Kim, Jayoung, Park, H., Ju, Y.S., Kim, E.-G., Kim, Jaehong, 2021. Cerebral Cavernous Malformation 1 Determines YAP/TAZ Signaling-Dependent Metastatic Hallmarks of Prostate Cancer Cells. Cancers 13, 1125. https://doi.org/10.3390/cancers13051125

Pietras, K., Östman, A., 2010. Hallmarks of cancer: Interactions with the tumor stroma. Exp. Cell Res. 316, 1324–1331. https://doi.org/10.1016/j.yexcr.2010.02.045

Playford, M.P., Schaller, M.D., 2004. The interplay between Src and integrins in normal and tumor biology. Oncogene 23, 7928–7946. https://doi.org/10.1038/sj.onc.1208080

Raza, A., Franklin, M.J., Dudek, A.Z., 2010. Pericytes and vessel maturation during tumor angiogenesis and metastasis. Am. J. Hematol. 85, 593–598. https://doi.org/10.1002/ajh.21745

Retta, S.F., Perrelli, A., Trabalzini, L., Finetti, F., 2020. From Genes and Mechanisms to Molecular-Targeted Therapies: The Long Climb to the Cure of Cerebral Cavernous Malformation (CCM) Disease, in: Trabalzini, L., Finetti, F., Retta, S.F. (Eds.), Cerebral Cavernous Malformations (CCM), Methods in Molecular Biology. Springer US, New York, NY, pp. 3–25. https://doi.org/10.1007/978-1-0716-0640-7_1

Reya, T., Morrison, S.J., Clarke, M.F., Weissman, I.L., 2001. Stem cells, cancer, and cancer stem cells. Nature 414, 105–111. https://doi.org/10.1038/35102167

Ridley, A.J., 2012. Historical overview of Rho GTPases. Methods Mol. Biol. Clifton NJ 827, 3–12. https://doi.org/10.1007/978-1-61779-442-1_1

Riento, K., Ridley, A.J., 2003. Rocks: multifunctional kinases in cell behaviour. Nat. Rev. Mol. Cell Biol. 4, 446–456. https://doi.org/10.1038/nrm1128

Riento, K., Villalonga, P., Garg, R., Ridley, A., 2005. Function and regulation of RhoE. Biochem. Soc. Trans. 33, 649–651. https://doi.org/10.1042/BST0330649

Saji, T., Nishita, M., Ikeda, K., Endo, M., Okada, Y., Minami, Y., 2022. c-Src–mediated phosphorylation and activation of kinesin KIF1C promotes elongation of invadopodia in cancer cells. J. Biol. Chem. 298, 102090. https://doi.org/10.1016/j.jbc.2022.102090

Sanz-Moreno, V., Gadea, G., Ahn, J., Paterson, H., Marra, P., Pinner, S., Sahai, E., Marshall, C.J., 2008. Rac Activation and Inactivation Control Plasticity of Tumor Cell Movement. Cell 135, 510–523. https://doi.org/10.1016/j.cell.2008.09.043

Sanz-Moreno, V., Marshall, C.J., 2010. The plasticity of cytoskeletal dynamics underlying neoplastic cell migration. Curr. Opin. Cell Biol. 22, 690–696. https://doi.org/10.1016/j.ceb.2010.08.020

Sasagawa, K., Matsudo, Y., Kang, M., Fujimura, L., Iitsuka, Y., Okada, S., Ochiai, T., Tokuhisa, T., Hatano, M., 2002. Identification of Nd1, a Novel Murine Kelch Family Protein, Involved in Stabilization of Actin Filaments. J. Biol. Chem. 277, 44140–44146. https://doi.org/10.1074/jbc.M202596200

Schäfer, M., Werner, S., 2008. Cancer as an overhealing wound: an old hypothesis revisited. Nat. Rev. Mol. Cell Biol. 9, 628–638. https://doi.org/10.1038/nrm2455

Serebriiskii, I., Estojak, J., Sonoda, G., Testa, J.R., Golemis, E.A., 1997. Association of Krev-1/rap1a with Krit1, a novel ankyrin repeat-containing protein encoded by a gene mapping to 7q21-22. Oncogene 15, 1043–1049. https://doi.org/10.1038/sj.onc.1201268

Serrels, B., Frame, M.C., 2012. FAK and talin: Who is taking whom to the integrin engagement party? J. Cell Biol. 196, 185–187. https://doi.org/10.1083/jcb.201112128

Shi, J., Wu, X., Surma, M., Vemula, S., Zhang, L., Yang, Y., Kapur, R., Wei, L., 2013. Distinct roles for ROCK1 and ROCK2 in the regulation of cell detachment. Cell Death Dis. 4, e483. https://doi.org/10.1038/cddis.2013.10

Smilenov, L.B., Mikhailov, A., Pelham, R.J., Marcantonio, E.E., Gundersen, G.G., 1999. Focal Adhesion Motility Revealed in Stationary Fibroblasts. Science 286, 1172–1174. https://doi.org/10.1126/science.286.5442.1172

Somlyo, A.V., Phelps, C., Dipierro, C., Eto, M., Read, P., Barrett, M., Gibson, J.J., Burnitz, M.C., Myers, C., Somlyo, A.P., 2003. Rho kinase and matrix metalloproteinase inhibitors cooperate to inhibit angiogenesis and growth of human prostate cancer xenotransplants. FASEB J. Off. Publ. Fed. Am. Soc. Exp. Biol. 17, 223–234. https://doi.org/10.1096/fj.02-0655com

Stockton, R.A., Shenkar, R., Awad, I.A., Ginsberg, M.H., 2010. Cerebral cavernous malformations proteins inhibit Rho kinase to stabilize vascular integrity. J. Exp. Med. 207, 881–896. https://doi.org/10.1084/jem.20091258

Su, V.L., Calderwood, D.A., 2020. Signalling through cerebral cavernous malformation protein networks. Open Biol. 10, 200263. https://doi.org/10.1098/rsob.200263

Sumi, T., Matsumoto, K., Nakamura, T., 2001. Specific activation of LIM kinase 2 via phosphorylation of threonine 505 by ROCK, a Rho-dependent protein kinase. J. Biol. Chem. 276, 670–676. https://doi.org/10.1074/jbc.M007074200

The UniProt Consortium, Bateman, A., Martin, M.-J., Orchard, S., Magrane, M., Ahmad, S., Alpi, E., Bowler-Barnett, E.H., Britto, R., Bye-A-Jee, H., Cukura, A., Denny, P., Dogan, T., Ebenezer, T., Fan, J., Garmiri, P., Da Costa Gonzales, L.J., Hatton-Ellis, E., Hussein, A., Ignatchenko, A., Insana, G., Ishtiaq, R., Joshi, V., Jyothi, D., Kandasaamy, S., Lock, A., Luciani, A., Lugaric, M., Luo, J., Lussi, Y., MacDougall, A., Madeira, F., Mahmoudy, M., Mishra, A., Moulang, K., Nightingale, A., Pundir, S., Qi, G., Raj, S., Raposo, P., Rice, D.L., Saidi, R., Santos, R., Speretta, E., Stephenson, J., Totoo, P., Turner, E., Tyagi, N., Vasudev, P., Warner, K., Watkins, X., Zaru, R., Zellner, H., Bridge, A.J., Aimo, L., Argoud-Puy, G., Auchincloss, A.H., Axelsen, K.B., Bansal, P., Baratin, D., Batista Neto, T.M., Blatter, M.-C., Bolleman, J.T., Boutet, E., Breuza, L., Gil, B.C., Casals-Casas, C., Echioukh, K.C., Coudert, E., Cuche, B., De Castro, E., Estreicher, A., Famiglietti, M.L., Feuermann, M.,

Gasteiger, E., Gaudet, P., Gehant, S., Gerritsen, V., Gos, A., Gruaz, N., Hulo, C., Hyka-Nouspikel, N., Jungo, F., Kerhornou, A., Le Mercier, P., Lieberherr, D., Masson, P., Morgat, A., Muthukrishnan, V., Paesano, S., Pedruzzi, I., Pilbout, S., Pourcel, L., Poux, S., Pozzato, M., Pruess, M., Redaschi, N., Rivoire, C., Sigrist, C.J.A., Sonesson, K., Sundaram, S., Wu, C.H., Arighi, C.N., Arminski, L., Chen, C., Chen, Y., Huang, H., Laiho, K., McGarvey, P., Natale, D.A., Ross, K., Vinayaka, C.R., Wang, Q., Wang, Y., Zhang, J., 2023. UniProt: the Universal Protein Knowledgebase in 2023. Nucleic Acids Res. 51, D523–D531. https://doi.org/10.1093/nar/gkac1052

Theisen, U., Straube, E., Straube, A., 2012. Directional Persistence of Migrating Cells Requires Kif1C-Mediated Stabilization of Trailing Adhesions. Dev. Cell 23, 1153–1166. https://doi.org/10.1016/j.devcel.2012.11.005

Thiery, J.P., 2002. Epithelial-mesenchymal transitions in tumour progression. Nat. Rev. Cancer 2, 442–454. https://doi.org/10.1038/nrc822

Totsukawa, G., Yamakita, Y., Yamashiro, S., Hartshorne, D.J., Sasaki, Y., Matsumura, F., 2000. Distinct roles of ROCK (Rho-kinase) and MLCK in spatial regulation of MLC phosphorylation for assembly of stress fibers and focal adhesions in 3T3 fibroblasts. J. Cell Biol. 150, 797–806. https://doi.org/10.1083/jcb.150.4.797

Tovchigrechko, A., Vakser, I.A., 2006. GRAMM-X public web server for protein-protein docking. Nucleic Acids Res. 34, W310–W314. https://doi.org/10.1093/nar/gkl206

Trezza, A., Geminiani, M., Cutrera, G., Dreassi, E., Frusciante, L., Lamponi, S., Spiga, O., Santucci, A., 2024. A Drug Discovery Approach to a Reveal Novel Antioxidant Natural Source: The Case of Chestnut Burr Biomass. Int. J. Mol. Sci. 25, 2517. https://doi.org/10.3390/ijms25052517

Wang, X., Enomoto, A., Weng, L., Mizutani, Y., Abudureyimu, S., Esaki, N., Tsuyuki, Y., Chen, C., Mii, S., Asai, N., Haga, H., Ishida, S., Yokota, K., Akiyama, M., Takahashi, M., 2018. Girdin/GIV regulates collective cancer cell migration by controlling cell adhesion and cytoskeletal organization. Cancer Sci. 109, 3643–3656. https://doi.org/10.1111/cas.13795

Webb, D.J., Donais, K., Whitmore, L.A., Thomas, S.M., Turner, C.E., Parsons, J.T., Horwitz, A.F., 2004. FAK-Src signalling through paxillin, ERK and MLCK regulates adhesion disassembly. Nat. Cell Biol. 6, 154–161. https://doi.org/10.1038/ncb1094

Wheeler, A., Ridley, A., 2004. Why three Rho proteins? RhoA, RhoB, RhoC, and cell motility. Exp. Cell Res. 301, 43–49. https://doi.org/10.1016/j.yexcr.2004.08.012

Wu, J., Jiang, J., Chen, B., Wang, K., Tang, Y., Liang, X., 2021. Plasticity of cancer cell invasion: Patterns and mechanisms. Transl. Oncol. 14, 100899. https://doi.org/10.1016/j.tranon.2020.100899

Wu, J.-S., Sheng, S.-R., Liang, X.-H., Tang, Y.-L., 2017. The role of tumor microenvironment in collective tumor cell invasion. Future Oncol. Lond. Engl. 13, 991–1002. https://doi.org/10.2217/fon-2016-0501

Xiao, Y., Yu, D., 2021. Tumor microenvironment as a therapeutic target in cancer. Pharmacol. Ther. 221, 107753. https://doi.org/10.1016/j.pharmthera.2020.107753

Yeatman, T.J., 2004. A renaissance for SRC. Nat. Rev. Cancer 4, 470–480. https://doi.org/10.1038/nrc1366

Zawistowski, J.S., Serebriiskii, I.G., Lee, M.F., Golemis, E.A., Marchuk, D.A., 2002. KRIT1 association with the integrin-binding protein ICAP-1: a new direction in the elucidation of cerebral cavernous malformations (CCM1) pathogenesis. Hum. Mol. Genet. 11, 389–396. https://doi.org/10.1093/hmg/11.4.389

Zawistowski, J.S., Stalheim, L., Uhlik, M.T., Abell, A.N., Ancrile, B.B., Johnson, G.L., Marchuk, D.A., 2005. CCM1 and CCM2 protein interactions in cell signaling: implications for cerebral cavernous malformations pathogenesis. Hum. Mol. Genet. 14, 2521–2531. https://doi.org/10.1093/hmg/ddi256

Zhang, J., 2001. Interaction between krit1 and icap1alpha infers perturbation of integrin beta1-mediated angiogenesis in the pathogenesis of cerebral cavernous malformation. Hum. Mol. Genet. 10, 2953–2960. https://doi.org/10.1093/hmg/10.25.2953

Zhang, J., Rigamonti, D., Dietz, H.C., Clatterbuck, R.E., 2007. Interaction between krit1 and malcavernin: implications for the pathogenesis of cerebral cavernous malformations. Neurosurgery 60, 353–359; discussion 359. https://doi.org/10.1227/01.NEU.0000249268.11074.83

Zhou, J., Zhu, Y., Zhang, G., Liu, N., Sun, L., Liu, M., Qiu, M., Luo, D., Tang, Q., Liao, Z., Zheng, Y., Bi, F., 2011. A distinct role of RhoB in gastric cancer suppression. Int. J. Cancer 128, 1057–1068. https://doi.org/10.1002/ijc.25445

Zhou, M., Yao, Y., Wang, X., Zha, L., Chen, Y., Li, Y., Wang, M., Yu, C., Zhou, Y., Li, Q., Cao, Z., Wu, J., Shi, S., Jiang, D., Long, D., Wang, J., Wang, Q., Cheng, X., Liao, Y., Tu, X., 2023. Crosstalk between KIF1C and PRKAR1A in left atrial myxoma. Commun. Biol. 6, 724. https://doi.org/10.1038/s42003-023-05094-5

Ziegler, W.H., Gingras, A.R., Critchley, D.R., Emsley, J., 2008. Integrin connections to the cytoskeleton through talin and vinculin. Biochem. Soc. Trans. 36, 235–239. https://doi.org/10.1042/BST0360235

8. LIST OF PUBLICATIONS

1. E. Ermini, A. Brai, E. Cini, F. Finetti, G. Giannini, D. Padula, L. Paradisi, F. Poggialini, L. Trabalzini, P. Tolu, M. Taddei. "A novel bioresponsive self-immolative spacer based on aza-quinone methide reactivity for the controlled release of thiols, phenols, amines, sulfonamides or amides" Chem Sci. (2024) 15(16), 6168-6177.

2. F. Finetti, L. Paradisi, C. Bernardi, M. Pannini, L. Trabalzini. "Cooperation between Prostaglandin E2 and Epidermal Growth Factor Receptor in Cancer Progression: A Dual Target for Cancer Therapy" Cancers (2023) 15(8), 2374.

3. F. Finetti, L. Paradisi, L. Trabalzini. "CCM proteins are key players in redox signaling and oxidative stress regulation in Cerebral Cavernous Malformations" Chapter 7 in "Pharmacological modulation of oxidative stress". Editors: Luciano Saso, Alessandro Giuffrè, Giuseppe Valacchi e Mauro Maccarrone (2023).

4. S. Fusi, G. Di Florio, N. Margiotta, A. Barbanente, E. Cini, F. Finetti, L. Paradisi, L. Trabalzini, F. Fabrizi de Biani, M. Corsini. "Synthesis, characterization, electrochemistry and in vitro cytotoxicity of a new "Triazole-Maltol" ligand and its platinum (II) complex" Inorganica Chimica Acta (2022) 532, 120756.